Polymer 51 (2010) 4015–4036

Contents lists available at ScienceDirect

Polymer

journal homepage: www.elsevier.com/locate/polymer

Feature Article

One-dimensional organic–inorganic hybrid nanomaterials

Jiayin Yuan [1], Axel H.E. Müller*

Makromolekulare Chemie II, Universität Bayreuth, D-95440 Bayreuth, Germany

ARTICLE INFO

Article history:
Received 20 April 2010
Received in revised form
24 June 2010
Accepted 25 June 2010
Available online 16 July 2010

Keywords:
Hybrids
Nanowires
Nanorods

ABSTRACT

This feature article presents the current research activities that concentrate on one-dimensional (1D) organic–inorganic hybrid nanostructures such as nanowires, nanorods, and nanotubes. The combination of organic and inorganic components in a 1D manner has been an increasingly expanding research field because the synergistic behavior of organic–inorganic materials is bound directly to the charming characteristics of 1D nanomaterials. These are responsible for the many novel optical and electrical properties, hierarchical superstructures, functions, and versatile applications that have been achieved. In this article, after justifying the interest in developing 1D organic–inorganic hybrid nanomaterials, we classify 1D hybrid nanostructures and review construction strategies that have been adopted, with a special focus on template-directed synthesis. In summary, we provide our personal perspectives on the future emphasis of the research on 1D organic–inorganic hybrid nanostructures.

1. Introduction

The pursuit of functional materials with novel properties and improved performance is a continually expanding research area that covers chemistry, physics, biology, and materials science. The largest activity in this field currently is the preparation, characterization, and application of nanomaterials where the constructing units have at least one dimension in the range from 1 to 100 nm. The interest in such structures mainly originates from the fact that novel properties as well as dramatically enhanced functions of materials are only acquired at this scale and – equally importantly – that these properties vary in size or shape, which is not a result of scaling factors [1]. In the past two decades, intensive research activities and corresponding fast progress in this field have indicated that the unique behavior of nanomaterials offers promising solutions to some crucial problems and challenges facing society such as sustainable energy (conversion, storage, and saving) [2–7], information storage [8–11] water treatment [12–14], and global warming [15–18].

Among the various explored nanostructures, the study of one-dimensional (1D) nanomaterials such as wires, rods, and tubes has entered a period of fast development within the past several years, and is presently the focus of many research groups [19–26]. The exploration of their unique properties determined by their size, 1D shape, and mutual interaction, and the challenges associated with their synthesis and fabrication, have stirred great interest and excitement. These anisotropic nanostructures are expected to play an important role as both building blocks, interconnects, and functional units in fabricating electronic, optoelectronic, electrochemical, and electromechanical nanoscale devices, for instance, waveguides [27], lasers [28], and nanogenerators [4]. At the nanoscale, the combination of active organic and inorganic components represents a new and immense area of materials science, which will have tremendous effects on the design and development of materials with well-defined functions or multifunctions.

Generally, the interest and demand for 1D organic–inorganic hybrid nanomaterials comes from the following factors. First, compared with their inorganic counterparts, many 1D hybrid nanomaterials possess improved colloidal stability by passivating the 1D inorganic surface, reducing the surface tension, and even solubilizing them in solution. In fact, this is the initial motivation for introducing organic molecules to inorganic nanostructures, since the stability in most cases is the primary request for future practical applications. In addition, coating 1D inorganic nanostructures with large molecules such as polymers enables the easy processing and addressing of individual nanostructures because the inorganic objects are shielded from each other by the thick polymer layer on their surfaces. This stabilizing effect is more obvious in solution, because the shell polymers tethered to a 1D object repel each other through steric or electrostatic repulsion. This is crucial for the fabrication of nanodevices from a single 1D object.

* Corresponding author. Tel.: +49 921 553399; fax: +49 921 553393.
E-mail address: Axel.mueller@uni-bayreuth.de (A.H.E. Müller).
[1] Present address: Max-Planck-Institut für Kolloid- und Grenzflächenforschung, D-14476 Potsdam, Germany.

0032-3861
doi:10.1016/j.polymer.2010.06.064

Second, by combining a judicious choice of organic and inorganic components in a controlled manner, the complexity and functionality of the 1D framework can be considerably enhanced. The synergetic relationship between the organic and inorganic parts can broaden the application field of 1D nanomaterials. For instance, a toxic 1D inorganic structure cannot realize its optical or electronic function without damaging the organism unless its surface is coated with biocompatible polymers or biomacromolecules. Besides, the stimuli-responsive behavior of some polymers can be incorporated into the inorganic 1D structure to make them "smart" and suitable for the task where feedback to external environment variations is needed.

Third, new properties and hierarchical architectures of 1D nanomaterials, which do not exist in any building block, can be attained through the interfacial interaction among the organic and/or inorganic phases in the 1D hybrid. It is not a fact of accumulating functions or properties into a single structure but of creating new ones in a synergistic way. For instance, when 1D hybrid nanomaterials are made from an artificial block "copolymer," in which one block is inorganic, they form elongated or curved superstructures because of the phase separation between the organic and inorganic parts.

Fourth, in some cases, an obvious advantage of 1D hybrids over 1D inorganic nanomaterials is that they are easy to scale up, because the organic phase of 1D hybrid nanomaterials facilitates a low-cost production, for example, in template-directed synthesis and electrospinning. Finally, 1D organic–inorganic nanostructures are often necessary as an intermediate for the preparation of pure inorganic or organic materials, especially in the case of porous 1D objects with ultralarge surface areas. The pores are formed when the organic or inorganic phases in the 1D hybrid are selectively etched away or degraded to leave nanoscale voids.

2. Structures of 1D organic–inorganic hybrid nanomaterials

In terms of the composition, architectures, and arrangement of the organic and inorganic species, 1D organic–inorganic hybrid nanomaterials exist mainly in the following groups (Fig. 1). The most simple and basic structure is a homogeneous organic–inorganic hybrid nanomaterial (Fig. 1A), in which the inorganic phase is evenly dissolved in the organic part at a molecular level [29]. A nanosized agglomeration of the inorganic phase is undetectable. This hybrid structure, often as an intermediate product of 1D inorganic nanostructures, is formed when metal ions are homogeneously bound in the organic phase before the further conduction of chemical reactions (e.g., reduction, sulfidation, or calcinations). Other types of 1D hybrid nanomaterials exhibit the phase separation of the inorganic or organic part of the nanoscale in their structures. Depending on the distribution of the nanosized inorganic or organic domains, core–shell-type (Fig. 1B), scattered-type (Fig. 1C, scattered phase in the entirety, core, or shell), and di-/tri-/multiblock structured 1D hybrids (Fig. 1D) have been reported. The spatial relationship of the inorganic and organic phases not only determines the intrinsic properties and functions of the corresponding hybrid, but also relates directly to different synthetic strategies, which will be introduced in the next chapter. Superstructures based on the combination of these basic groups are also possible. For example, the organic or inorganic block in structures B and D can be substituted by a hybrid block. Since the research activities in this field are still in progress, new structures and architectures are expected to appear in the future.

3. Synthetic strategies

Compared with spherical nanoparticles, the development of 1D hybrid nanomaterials came with an appreciable delay during the 1990s. This is because the elongated structures restricted within one direction are generally not energetically favored. Although carbon nanotubes (CNTs), as the most intensively researched 1D nanostructure, were reported in 1991 [30], the preparation of 1D hybrid nanomaterials has been hampered as a result of the difficult shape control and phase distribution at an extremely small size. To favor the anisotropic growth of the materials at the nanoscale, physically or chemically forced and oriented growth conditions are required to satisfy the structure extension. Within the past several years, benefiting from the pioneering work of Lieber, Xia, Yang, and others in the field of 1D inorganic nanostructures [19,22,24,27,28], 1D hybrids have attracted more and more attention. Initial efforts have aimed to handle their preparation and explore their unusual properties. Many methods have so far been used to prepare and fabricate 1D organic–inorganic hybrid nanomaterials including template-directed synthesis, electrospinning, oriented attachment, and others.

3.1. Template-directed synthesis

Of all preparation methods, the template-directed method is the most facile and frequently used. It allows the direct transfer of a desired (often complex) topology given by the inner or outer surface of a template, and thereby is a conceptually simple, intuitive, straightforward, and versatile route to 1D hybrid nanostructures. Templates, based on how they are formed, can be divided into several groups, including mesoscale structures self-assembled from surfactants or block copolymers, unimolecular cylindrical polymer brushes (CPBs), biological superstructures such as DNA and viruses, channels within solid polymeric or inorganic materials, and other existing 1D objects (Fig. 2). According to their physical state, they can also be classified into two types: "soft" and "hard" ones. Typically, organic compounds including polymers are used as soft templates. The soft template can remain in the final hybrid to achieve a specific goal, for example, avoiding agglomeration. It can also be eliminated by calcination at an elevated temperature or extraction with a solvent to render pure inorganic materials. Hard templates are made up of rigid materials such as channels in solids. The apparent advantage of a hard template is its superior control over the size and uniformity of the 1D

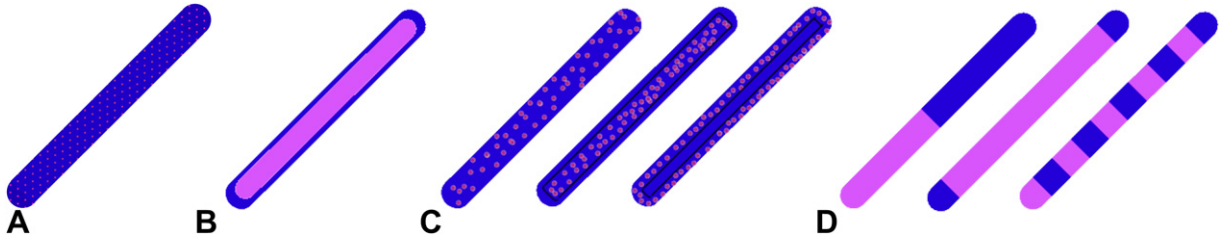

Fig. 1. Illustration of 1D organic–inorganic hybrid nanostructures.

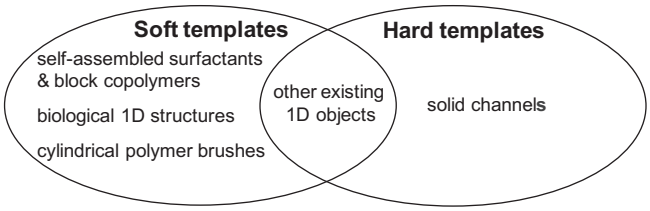

Fig. 2. Classification of templates for the fabrication of 1D hybrids.

nanostructures to be prepared. This is of huge importance when the size effect is the main interest in the research. However, compared with soft templates, the weakness of using hard templates lies in the template preparation, which is often expensive and difficult to scale up.

3.1.1. Self-assembled mesostructures from surfactants or block copolymers

3.1.1.1. Surfactant micelles. It is well known that surfactant molecules can spontaneously organize into rod-like micelles (or inverse micelles) when their concentration reaches a critical value [31]. These anisotropic structures can be immediately, or after fixation, used as soft templates to promote the formation of nanowires, nanorods, or nanotubes when coupled with an appropriate chemical reaction. This route is useful to prepare metal or metal oxide nanorods in solution. Murphy and co-workers demonstrated the seed-mediated growth of gold nanorods in a solution that contained rod-like micelles assembled from cetyltrimethylammonium bromide (CTAB) [32,33]. The lateral dimensions and aspect ratios of these nanorods could be controlled by varying the ratio of seeds relative to the metal precursors. The surfactants stabilize the formed nanorods in aqueous solution through electrostatic repulsion. In some special cases, surfactants can be also deeply incorporated into the nanorod entity, leading to pore structures in the nanorod after the removal of surfactants. For instance, α-FeOOH nanorods with diameters of 170–210 nm and lengths up to 3–5 μm were synthesized in a high yield via hydrothermal methods using worm-like micelles of sodium dodecyl sulphate (SDS) as templates (Fig. 3) [34]. The surfactants were sequentially removed from the α-FeOOH nanorods to provide the porous rod morphology. From a mass point of view, the surfactants on the nanorods or nanowires make up only a very tiny portion of the whole mass. Thus the formed 1D nanostructures are often considered inorganic; however, when their practical applications are closely related to the surface chemistry, their hybrid nature should be seriously considered. In the case of ultrathin nanowires (2–3 nm), the importance of surface chemistry is especially amplified compared with thicker ones [20].

3.1.1.2. Block copolymer micelles in solution. Compared with small organic molecules, block copolymers represent versatile and powerful soft templates for the fabrication of hybrid nanomaterials with hierarchical architectures and complex functionalities. By means of self-assembly, either concentration-driven or induced by external stimuli such as temperature or solvent selectivity, block copolymers can undergo microphase segregation to give various morphologies (micelles, vesicles, rods, and tubes) in solution. Owing to dissimilar physical and chemical properties, the compartments of different polymer chains can be separately addressed by the decoration of inorganic materials. As early as the 1990s, Möller et al. demonstrated that spherical micelles formed from diblock copolymers in a selective solvent could precisely control the mineralization of metals in the micelle core of a nanometer scale [35–37]. By employing cylindrical micelles that are formed from block copolymers with suitable volume fractions in solution, 1D hybrids can be straightforwardly prepared by loading inorganic moieties. Eisenberg et al. reported that a loose necklace of cadmium sulfide (CdS) quantum dots (QDs) was formed within poly(ethylene oxide)-*block*-polystyrene-*block*-poly(acrylic acid) (PEO-*b*-PS-*b*-PAA) triblock terpolymer worm-like micelles in tetrahydrofuran (THF) [38]. The cylindrical structures were obtained via the self-assembly of the triblock terpolymer in the presence of Cd^{2+} ions. Coordination between the Cd^{2+} ions and the PAA block led to ionically crosslinked primary worm-like micelles consisting of a cadmium polyacrylate core, a PS shell, and a PEO corona. The Cd^{2+} ions were subsequently converted into CdS nanoparticles in the cylindrical core by reacting with H_2S gas.

An alternative way to make 1D hybrids based on polymeric materials is to directly assemble inorganic precursor-containing block copolymers in solution. For example, one block can be constructed by a monomer containing an inorganic precursor. In this manner, the copolymer itself is already a hybrid material; the remaining task is to have these copolymers arranged in an extended conformation in solution, i.e., the self-assembly process of

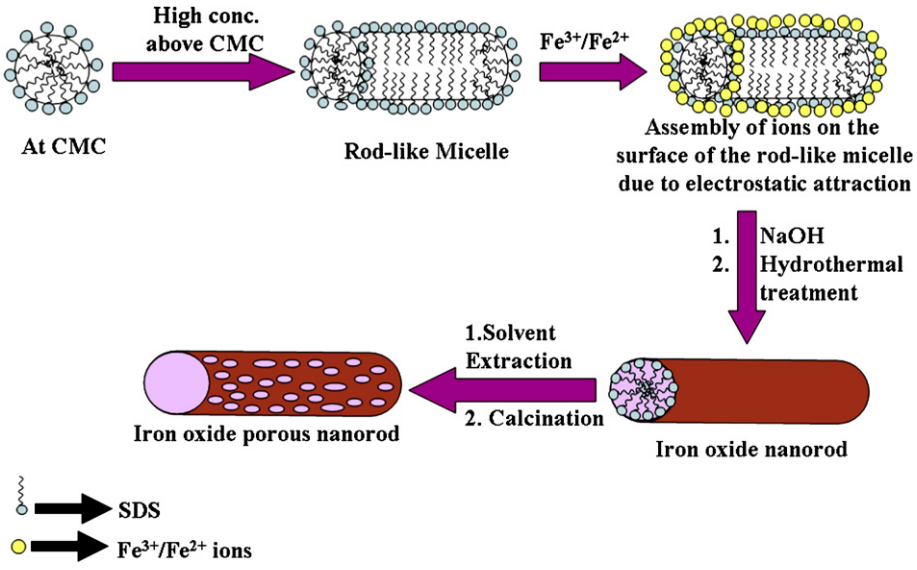

Fig. 3. Synthesis of α-FeOOH and α-Fe_2O_3 nanorods in aqueous SDS solution [34]. Reprinted with the permission of Elsevier.

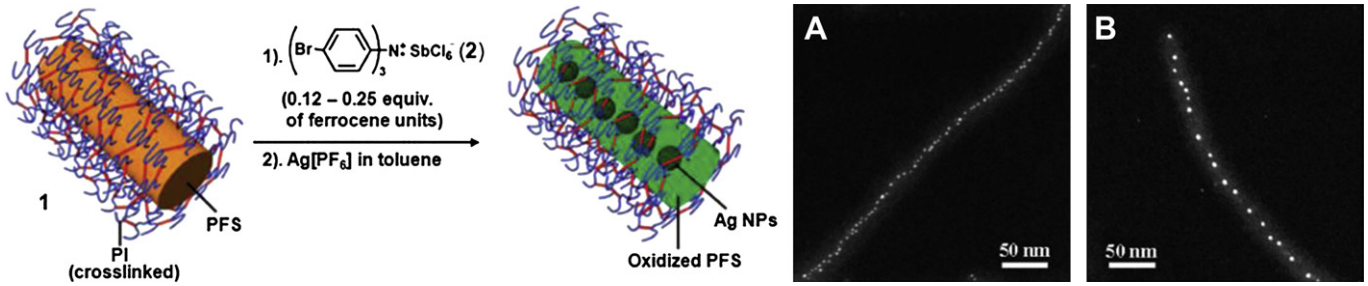

Fig. 4. Left: synthetic route to the encapsulation of silver nanoparticles in shell-crosslinked PI-*b*-PFS hybrid cylindrical micelles. Right: dark-field TEM images of silver nanoparticles doped shell-crosslinked PI-*b*-PFS hybrid cylinders after the addition of $Ag[PF_6]$ in different amounts: 12.5% (A) and 25% (B) for total ferrocene units [50]. Reprinted with the permission of ACS.

organometallic block copolymers is accomplished simultaneously with the 1D alignment of the inorganic moieties. Winnik and Manners carried out pioneering research in polymerizing various iron-containing monomers, such as [1] di(n-butyl)germaferrocenophane and ferrocenyldimethylsilane [39–57]. The common characteristic of these corresponding polymers is their ability to crystallize into rod-like objects. As an example, poly(ferrocenyldimethylsilane) (PFS), possessing interacting Fe and Si atoms along the polymer main chain, is a semicrystalline polymer. When it is associated with another polymer, such as poly(dimethylsiloxane) (PDMS), PS, poly(2-vinylpyridine) (P2VP), or polyisoprene (PI) to form a diblock copolymer, colloidally stable cylindrical micelles with the PFS block in the core are formed. The energetic driving force for the formation of such cylindrical micelles lies in the crystallization of the PFS block. The self-assembled cylindrical micelles themselves are 1D hybrid nanomaterials. The fascinating properties of these hybrid micelles is that more complex 1D hybrid nanostructures can be easily constructed from them. In one case, they served as a template for the deposition of various inorganic nanoparticles. For example, PI-*b*-PFS cylinders were applied as the 1D template to encapsulate silver nanoparticles by first crosslinking the hydrophobic PI shell and then *in situ* reducing the silver ions into nanoparticles inside the cylinders (Fig. 4) [50]. In another example, silica, zirconia, alumina, titania, and magnetite nanoparticles were homogeneously incorporated into the P2VP corona of PFS-*b*-P2VP cylinder micelles, forming a 1D hybrid superstructure with a iron-containing core and a hybrid corona possessing the corresponding inorganic moiety [56]. Furthermore, because of the living nature of this self-assembly process, a unique type of ABA triblock co-micelles were generated. The spatially selective decoration of the middle block of the triblock co-micelles with titania results in ABA-type segmented 1D hybrid nanostructures.

Combining the living characteristics of the self-assembly process and the variety of monomers used to build the cylindrical

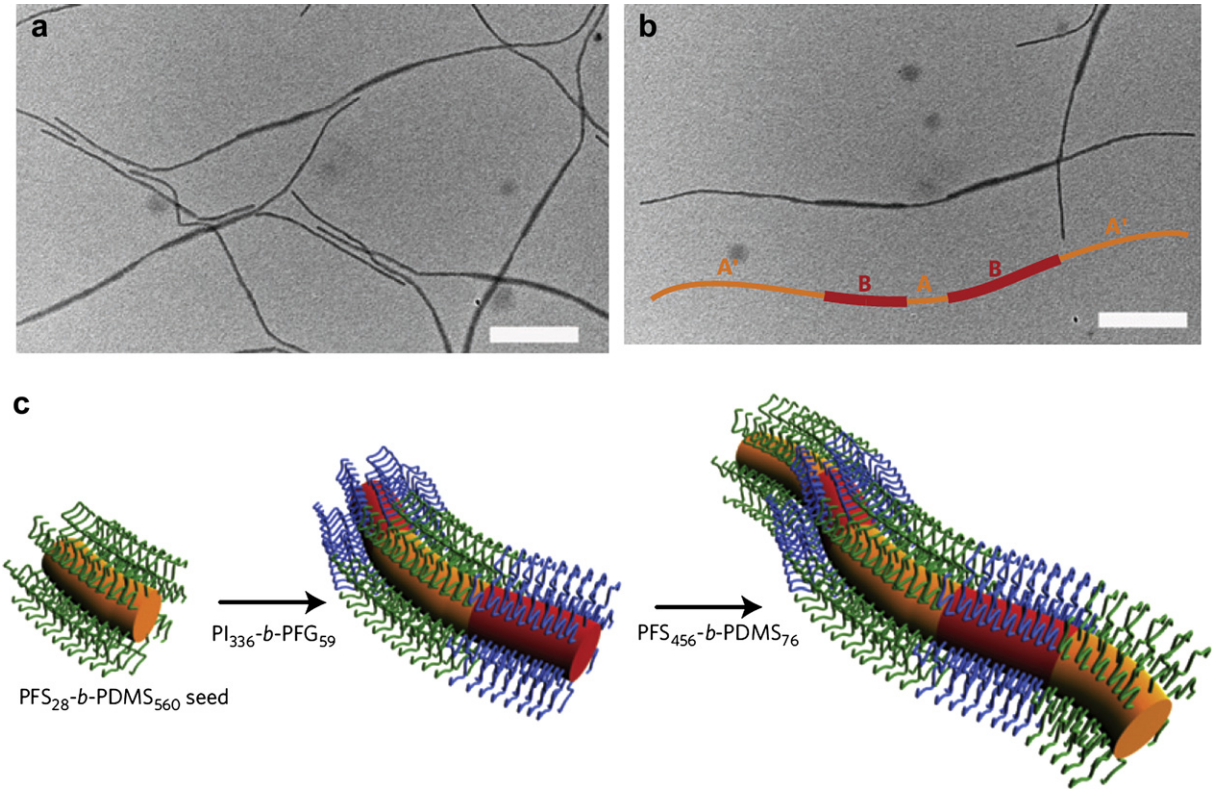

Fig. 5. TEM micrographs of heteroepitaxially grown pentablock co-micelles. (a, b) Pentablock co-micelles M(PFS_{456}-*b*-$PDMS_{76}$)-*b*-M(PI_{336}-*b*-PFG_{59})-*b*-M(PFS_{28}-*b*-$PDMS_{560}$)-*b*-M(PI_{336}-*b*-PFG_{59})-*b*-M(PFS_{456}-*b*-$PDMS_{76}$) (scale bars: 500 nm). (c) Schematic representation of the formation of pentablock co-micelles with different core-forming blocks (blue corona indicates PI, green corona indicates PDMS) [57]. Reprinted with the permission of Nature Publishing Group.

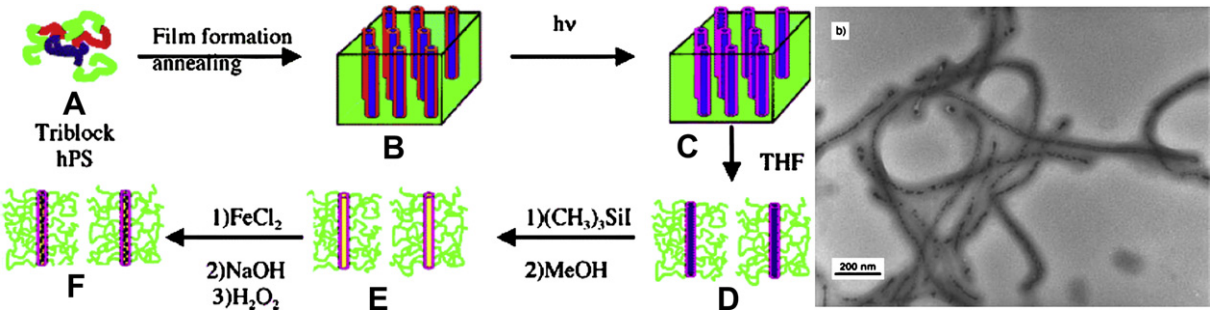

Fig. 6. Synthetic strategy (left) and TEM image (right) of the PS-*b*-PCEMA-*b*-PAA triblock copolymer/γ-Fe_2O_3 hybrid magnetic nanofibers [70]. Reprinted with the permission of Wiley-VCH.

micellar core, an alternating multiblock 1D hybrid hierarchical superstructure is possible [57]. A hybrid cylindrical micelle, assembled from PFS_{28}-*b*-$PDMS_{560}$ diblock copolymers, has been used as a monoblock seed for the crystallization-driven growth of the PI_{336}-*b*-PFG_{59} (PFG: poly(ferrocenyldimethylgermane)) diblock copolymer on both ends (Fig. 5). This leads to a heteroepitaxial ABA block co-micelle, which is also an ABA triblock cylindrical co-micelle hybrid object. The seed-mediated growth continues from its two ends in the presence of the PFS_{456}-*b*-$PDMS_{76}$ diblock copolymer, expanding the triblock to alternating pentablock heteroepitaxial hybrid co-micelles.

3.1.1.3. Block copolymer self-assembly in the bulk. Block copolymers are powerful tools to control the ordering or packing of inorganic nanodomains in a dense and periodic manner either in the bulk or on solid substrates. For example, Möller et al. reported the preparation of hexagonally ordered metallic nanodots on several substrates by transferring metal-loaded inverse micelles onto substrates [58–62]. Russell et al. demonstrated various possibilities to obtain well-ordered inorganic nanodots or nanowires derived from self-assembled block copolymers as soft template on solid substrates [63–67]. Very recently, Fahmi et al. synthesized gold nanoparticles located within the P4VP domains (either cylindrical or lamellar-like) of a PS-b-P4VP diblock copolymer in the solid state through the selective incorporation of $HAuCl_4$ to the pyridine groups in the P4VP block [68,69].

Morphologies obtained from block copolymer self-assembly in the bulk (in particular cylindrical or tubular ones) can be locked by crosslinking reactions and transferred into solution. These structures have been used as templates for colloidally stable 1D hybrids. Liu and co-workers [70–72] synthesized crosslinked cylindrical polymer assemblies starting from a linear triblock terpolymer polystyrene-*b*-poly(2-cinnamoylethyl methacrylate)-*b*-poly(*tert*-butyl acrylate) (PS-*b*-PCEMA-*b*-P*t*BA) in the solid state (Fig. 6). The triblock terpolymer initially self-assembled into an array of core–shell cylinders with a P*t*BA core and a PCEMA shell. The latter was further photo-crosslinked in the bulk. Upon interaction with a good solvent for the polymer, the crosslinked fibers were dispersed into solution, which in the following step were converted into nanotubes with interior carboxylic acid groups by the selective hydrolysis of P*t*BA into PAA, a weak polyelectrolyte capable of coordinating metal ions. By the encapsulation of inorganic nanoparticles such as *in situ*-generated γ-Fe_2O_3 within the polymeric nanotubes, well-defined 1D magnetic hybrids with good stability in solution and magnetic response were obtained [70].

Besides polymeric tubular templates, core crosslinked polybutadiene-*b*-poly(2-vinylpyridine) (PB-*b*-P2VP) block copolymer nanorods were used as a template for the synthesis of heteropolyoxometalate (POM) nanostructures by attaching $[SiMo_{12}O_{40}]^{4-}$ Keggin ions onto the P2VP corona of the template (Fig. 7) [73]. A PB-*b*-P2VP block copolymer with 30 wt% 1,2-PB formed PB cylinders embedded in the P2VP matrix. The unsaturated PB cores were crosslinked using a photointiator to lock the cylindrical structure. The core crosslinked cylinders exhibited worm-like morphologies when dissolved in THF or acetone. The produced POMs exhibited high dispersion and an improved surface area and are thereby expected to be useful in catalytic-, electrochemical-, and biotechnology-related applications.

Different from linear block copolymers, an SBV miktoarm star terpolymer bearing three different arms of PS, PB, and P2VP connected in one branching point was applied for the preparation of polymer–inorganic bidirectional hybrid nanowires with tunable structures by solvent replacement [74]. The polymeric template was prepared similarly by crosslinking the PB microdomain of the

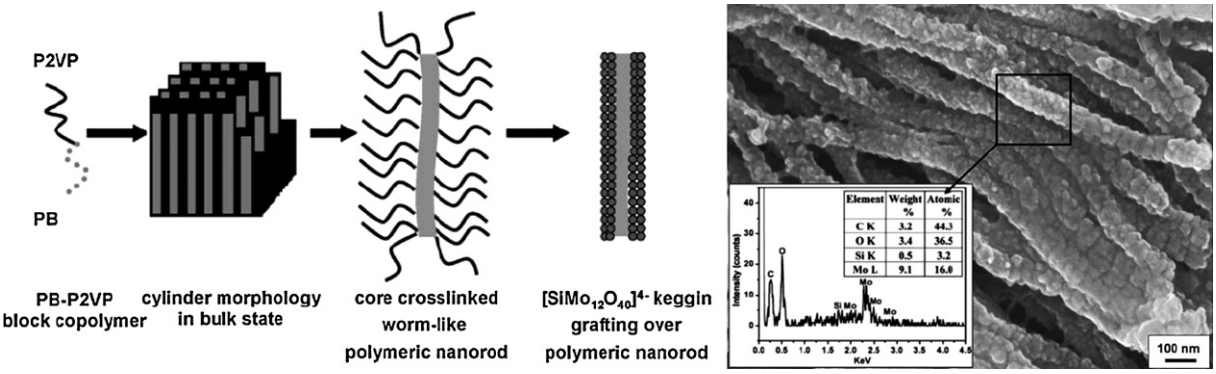

Fig. 7. Left: illustration of the synthesis of $[SiMo_{12}O_{40}]^{4-}$ Keggin ion nanostructures from the core crosslinked PB-*b*-P2VP worm-like polymer template and $[SiMo_{12}O_{40}]^{4-}$. Right: SEM image of the $[SiMo_{12}O_{40}]^{4-}$ POM grafted onto core crosslinked PB-*b*-P2VP worm-like polymer template (inset: energy dispersive X-ray analysis spectrum) [73]. Reprinted with the permission of RSC.

miktoarm star polymer in the bulk (Fig. 8). The asymmetric, ribbon-like PB domains (black) surrounded by two symmetric and opposing PS (red) and two P2VP (green) domains, respectively were then fixed. Subsequent dissolution using sonication allowed the transfer of this distinctive morphology from the bulk into solution and yielded a multicompartment cylinder (MCC). Bidirectional polymer–inorganic hybrid nanowires were formed by localizing transition metal or cadmium sulfide nanoparticles into the two opposite parallel P2VP cylindrical domains trapped in each single MCC. The resulting hybrid MCCs bore two perfectly parallel hybrid nanowires, which were tunable in terms of the distribution of the inorganic nanoparticles in the P2VP corona. The two limiting cases were (a) perfectly aligned, parallel hybrid nanowires in toluene (good solvent for PS and non-solvent for P2VP) and (b) nanotubes with one homogeneous hybrid corona in ethanol (non-solvent for PS and good solvent for P2VP).

Obviously, in terms of self-assembly, synthetic block copolymers, compared with surfactants, offer more complex architectures to create 1D hybrid materials of unprecedented complexities and desirable morphologies. This is because of the large number of existing monomers, fast development of the controlled/living polymerization techniques, and large number of available morphologies in the self-assembly process, in particular when three different blocks or non-linear topologies are involved. It is fascinating that in confined nanoscale channels, the self-assembly process appears different and leads to more complex and unusual architectures, which are ready as polymeric templates for the fabrication of 1D hybrid nanostructures [75].

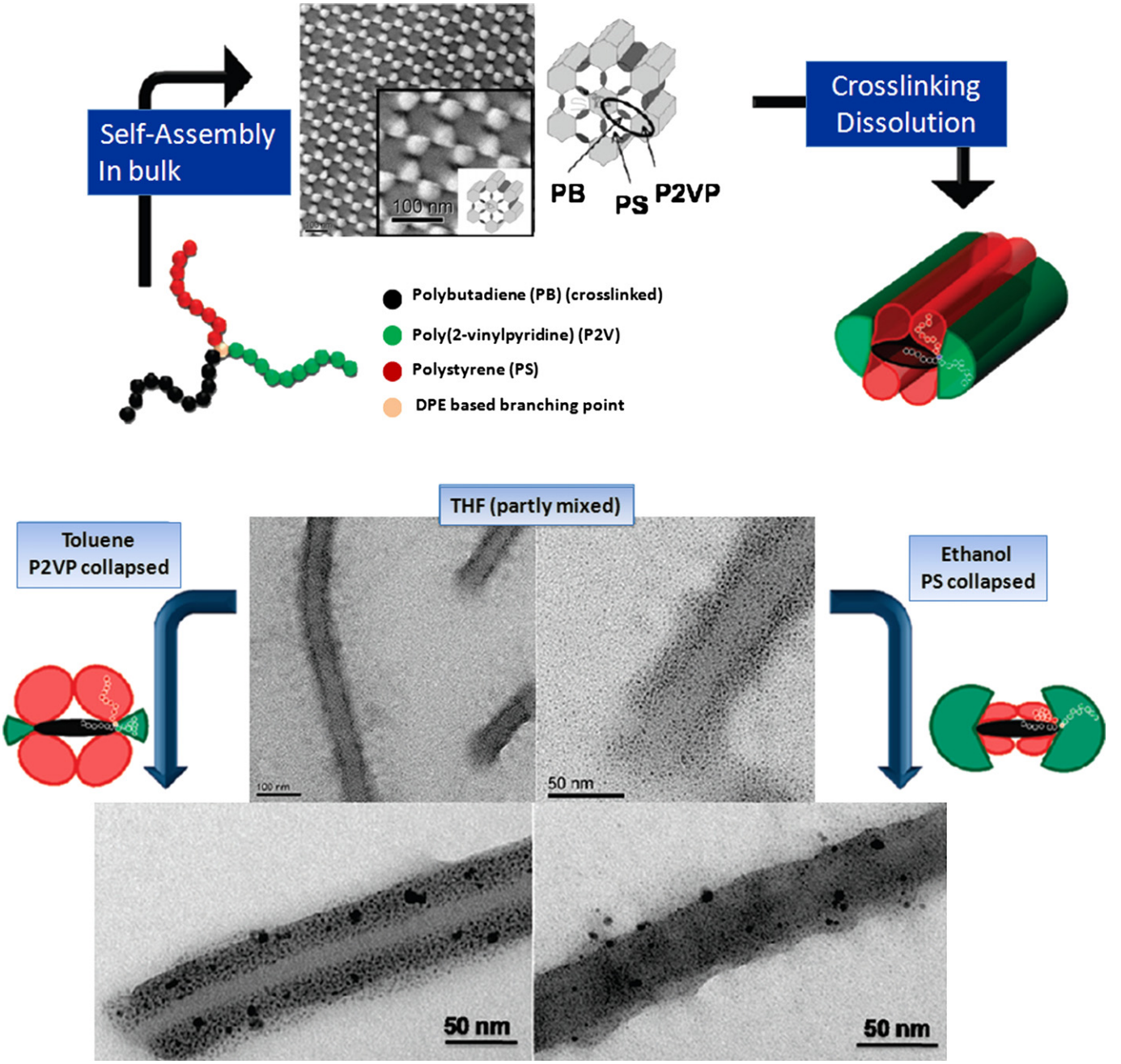

Fig. 8. Top: the center shows a TEM micrograph and the schematic representation of the hexagonal bulk structure stained with OsO_4 and I_2. Therein PB, P2VP, and PS appear black, gray, and white, respectively. Bottom: structural changes of the Ag-loaded corona upon exposure to selective solvents. TEM micrographs of Ag-loaded hybrid MCCs deposited from THF (top), toluene (lower left), and ethanol (lower right) [74]. Reprinted with the permission of ACS.

3.1.2. Unimolecular CPBs

Instead of polymeric templates constructed from the assembly of tens or hundreds of macromolecules, a unimolecular polymer template can be precisely designed and will linearly direct the inorganic moiety. CPBs, also known as "molecular bottlebrushes," possessing linear side chains or high-generation dendritic side groups densely grafted from a linear main chain, have been adopted as cylindrical templates because of their extended conformation based on the intramolecular excluded volume interactions between densely grafted side chains. They are synthesized by using "grafting from," "grafting onto," or "grafting though" strategies [76]. Among various structures, core–shell structured CPBs with diblock copolymer side chains are of special interest because the phase separation between the core and shell defines an interior cylindrical domain with a length up to several hundred nanometers. These are considered ideal nanoreactors to generate and spatially force inorganic nanoparticles in a 1D manner. A typical "grafting from" synthetic strategy for core–shell structured amphiphilic CPBs with a PAA core and a poly(*n*-butyl acrylate) (P*n*BA) shell is illustrated in Fig. 9. The whole macromolecule is prepared by the combination of atom transfer radical polymerization (ATRP) or anionic polymerization for the poly(2-hydroxyethyl methacrylate) (PHEMA) backbone and ATRP for the side chains, aiming at the strict dimensional control of the formed hybrids.

As a first attempt, core–shell CPBs with a hydrophilic P2VP core and a hydrophobic PS shell were employed as templates to prepare a linear array of gold nanoclusters and nanowires. In this synthesis, the P2VP domains were one-dimensionally confined by the PS corona and coordinated with $AuCl_4^-$ ions. After reduction by $NaBH_4$, gold nanoparticles were *in situ*-generated exclusively within the core and aligned linearly [77]. However, the length distribution of the template was very broad because they were synthesized using the "grafting through" method, i.e., the free radical polymerization of a PS-*b*-P2VP macromonomer.

A promising step towards the application of amphiphilic core–shell CPBs as templates for fabricating 1D hybrids with controlled length distribution was performed by grafting the side chains from the backbone ("grafting from" method) via ATRP. These were used as cylindrical unimolecular nanoreactors for the generation of 1D inorganic nanostructures, including wire-like assemblies of semiconducting (CdS, CdSe) nanoparticles and superparamagnetic maghemite (γ-Fe_2O_3) hybrid nanocylinders (Fig. 10A–F) [78–80]. This synthetic strategy takes advantage of each unique aspect of the CPBs. First, the PAA core of the polymer brush-possessing carboxylate groups is capable of undergoing coordination chemistry with metal ions (Cd^{2+}, Fe^{3+}, Fe^{2+}, etc.) and works as a nanoreactor for the nanoparticle formation. At the same time, it dimensionally directs the particle distribution along the brush backbone. Second, the P*n*BA shell of the polymer brush protects the fabricated 1D hybrids from aggregation and provides solubility in organic solvents. Another interesting characteristic of the CPBs with a PAA core is that after the formation of inorganic nanoparticles within the cylindrical core, the PAA chemical structure is recuperated, and thereby a second nanoparticle-loading process is feasible to enhance the inorganic fraction in the formed 1D hybrids. This possibility has been demonstrated in the preparation of CPB–CdSe hybrid nanowires. The UV spectra of the hybrid nanowires after the first and second loading processes have indicated an increasing intensity and red-shift of the threshold wavelength because of the further growth of the CdSe nanoparticles within the CPB core [63]. Very recently, core–shell bis-hydrophilic CPBs with a PHEMA core and a poly(oligo(ethylene glycol) methacrylate) (POEGMA) shell have been demonstrated to direct the controlled fabrication of linear assemblies of titania nanoparticles, forming titania–CPB hybrid nanowires [81]. The key challenge in using a bis-hydrophilic CPB as a template lies in the selective immobilization of the precursors in the core in spite of the hydrophilic shell. The aim is achieved by attaching Ti^{4+} ions firmly in the PHEMA core via a transalcoholysis-introduced covalent bond. The

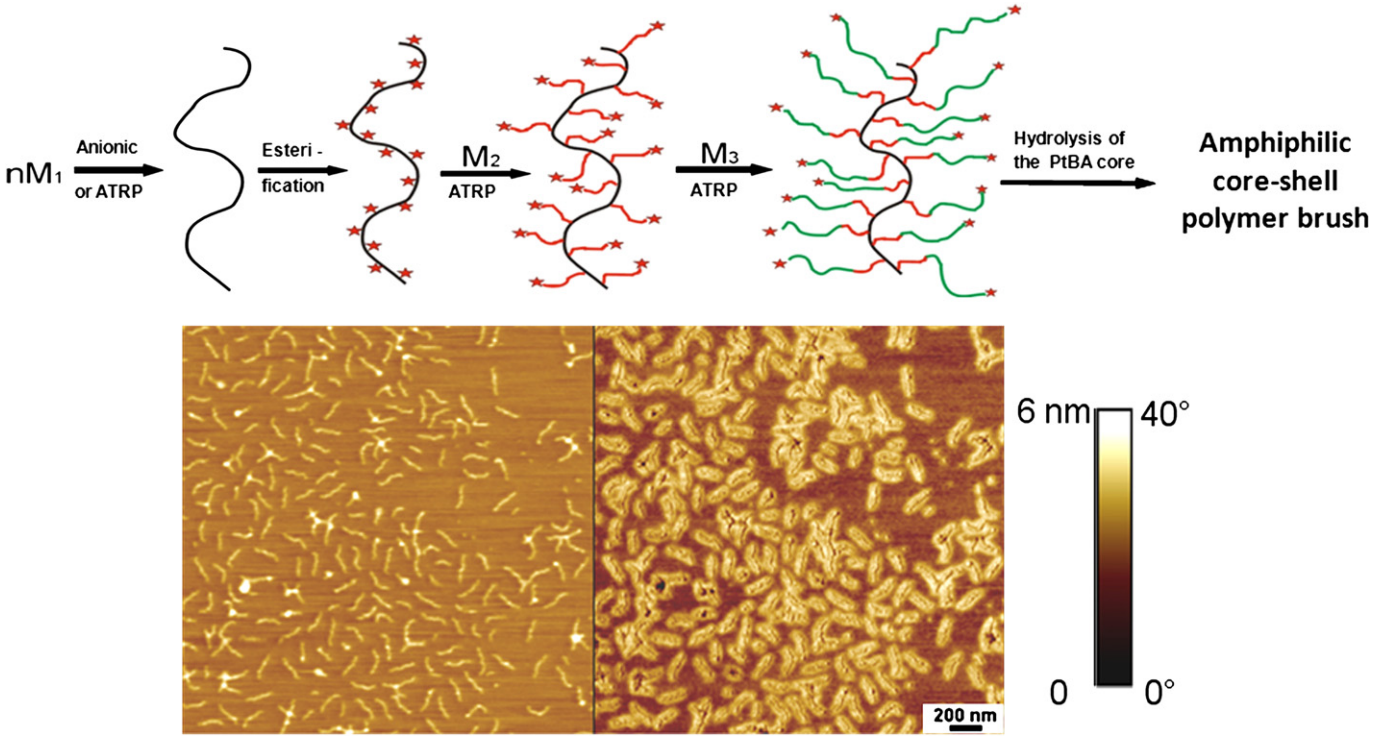

Fig. 9. Top: Synthetic route to a CPB with PAA-*b*-P*n*BA amphiphilic diblock copolymer side chains (M_1:HEMA or silyl-protected HEMA; M_2:*t*BA; M_3:*n*BA; asterisk:initiating site). Bottom: AFM images of core–shell polymer brushes ($[AA_{37}$-*b*-$nBA_{76}]_{1500}$) on a mica: height image (left) and phase image (right) [76]. Reprinted with the permission of Elsevier.

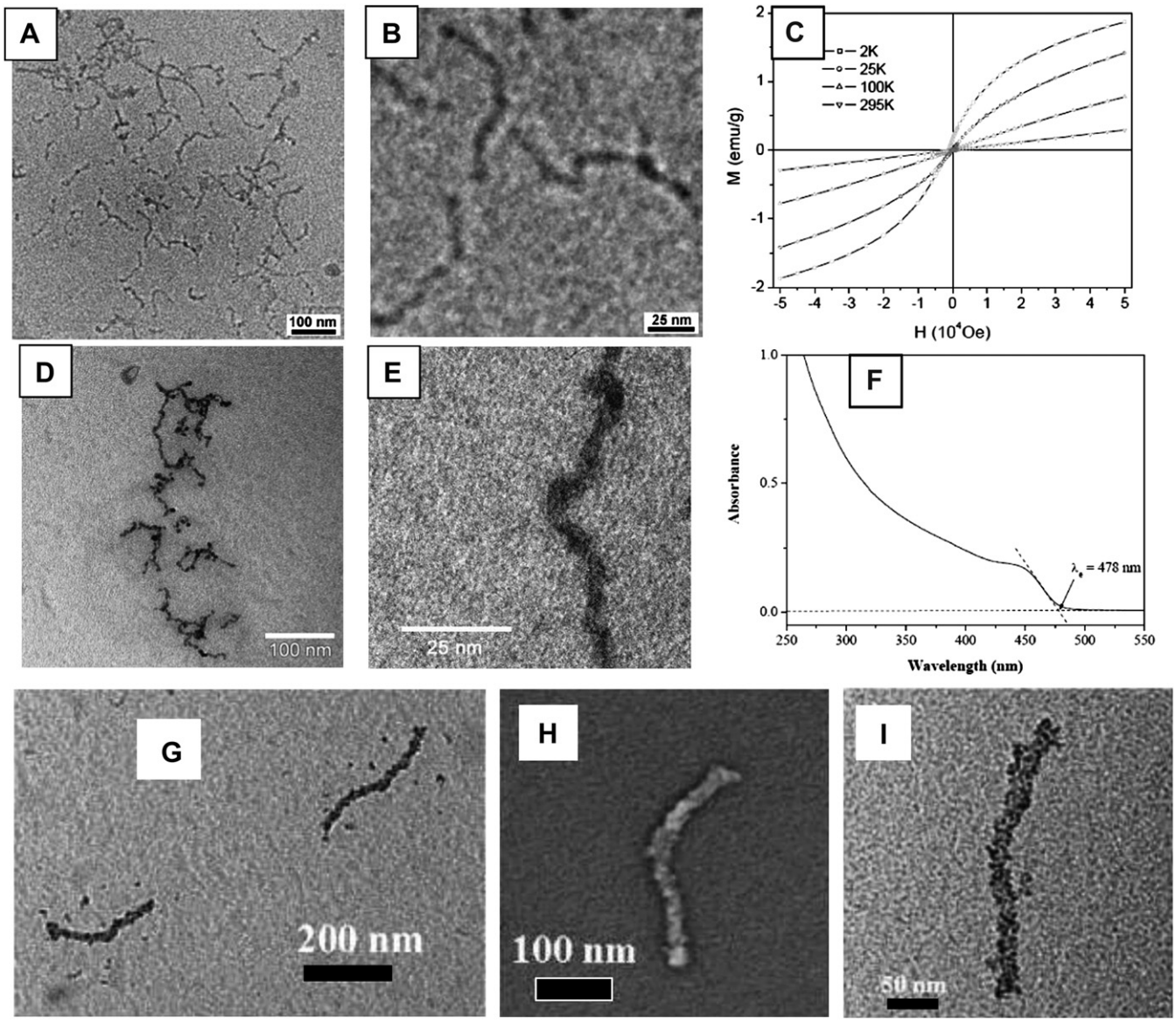

Fig. 10. (A) Non-stained TEM image of superparamagnetic γ-Fe_2O_3 hybrid nanowires templated by amphiphilic CPBs with a PAA core and a P*n*BA shell; (B) enlarged view; and (C) corresponding magnetization curve of the hybrid. (D) Non-stained TEM image of CdS hybrid nanowires; (E) enlarged view; and (F) corresponding UV–vis spectrum. (G) TEM image of CPB–Ti^{4+} hybrid nanowires. (H, I) SEM and TEM images of CPB–titania hybrid nanowires [78,79,81]. Reprinted with the permission of Wiley-VCH and ACS.

POEGMA shell only loosely complexes Ti^{4+} ions. This is confirmed by the TEM characterization of Ti^{4+}-doped CPBs in Fig. 10G, in which the black worm represents the PHEMA core (covalent bond with Ti^{4+}) and the scattered dots represents the POEGMA shell (loosely complexing Ti^{4+}). After hydrolyzing the Ti^{4+} ions, titania nanoparticles were found to be distributed evenly along the linear core. The titania moieties formed in the POEGMA shell are believed to have fused onto the titania nanoparticles in the core.

A different strategy in applying CPB as a template for the preparation of 1D organic–inorganic hybrid nanomaterials was recently made. In this approach, the inorganic precursor exists already as one block of the CPB side chain. Specifically, water-soluble organo-silica hybrid nanowires with a silsesquioxane ($RSiO_{1.5}$) core and a corona made up of oligo(ethylene glycol) methacrylate (OEGMA) were prepared (Fig. 11) [82]. The novelty in the synthetic route is the employment of a silicon-containing monomer, 3-acryloylpropyltrimethoxysilane (APTS), in which a trimethoxysilyl group (silica precursor) is linked to a polymerizable acrylate group. The silica precursor is then incorporated into the cylindrical core when the APTS and OEGMA monomers are sequentially polymerized from the poly(macroinitiator) backbone. Since no external silica precursor is added, the formation of free silica nanoparticles in the solution is totally excluded from this process. The POEGMA shell solubilizes them in various solvents, including water. The crosslinked silsesquioxane core makes the brushes rigid. Consequently, as a promising application, these hybrid silica nanowires show the ability to develop a lyotropic liquid crystalline phase at a higher concentration in a liquid thin film. In addition, the pyrolysis of the hybrid nanowires on a solid substrate leads to the formation of purely inorganic silica nanowires.

As mentioned above, superparamagnetic hybrid nanocylinders were prepared by the *in situ* generation of maghemite nanoparticles within CPBs with a PAA core and P*n*BA shell. Because of the amphiphilic nature of CPBs, organic solvent mixtures were used to disperse the hybrids, which were unstable in the long-term and inconvenient for applications. The magnetic nanoparticles generated *in situ* in the core of the CPBs were only 2–3 nm and the magnetic response was weak. In an improved

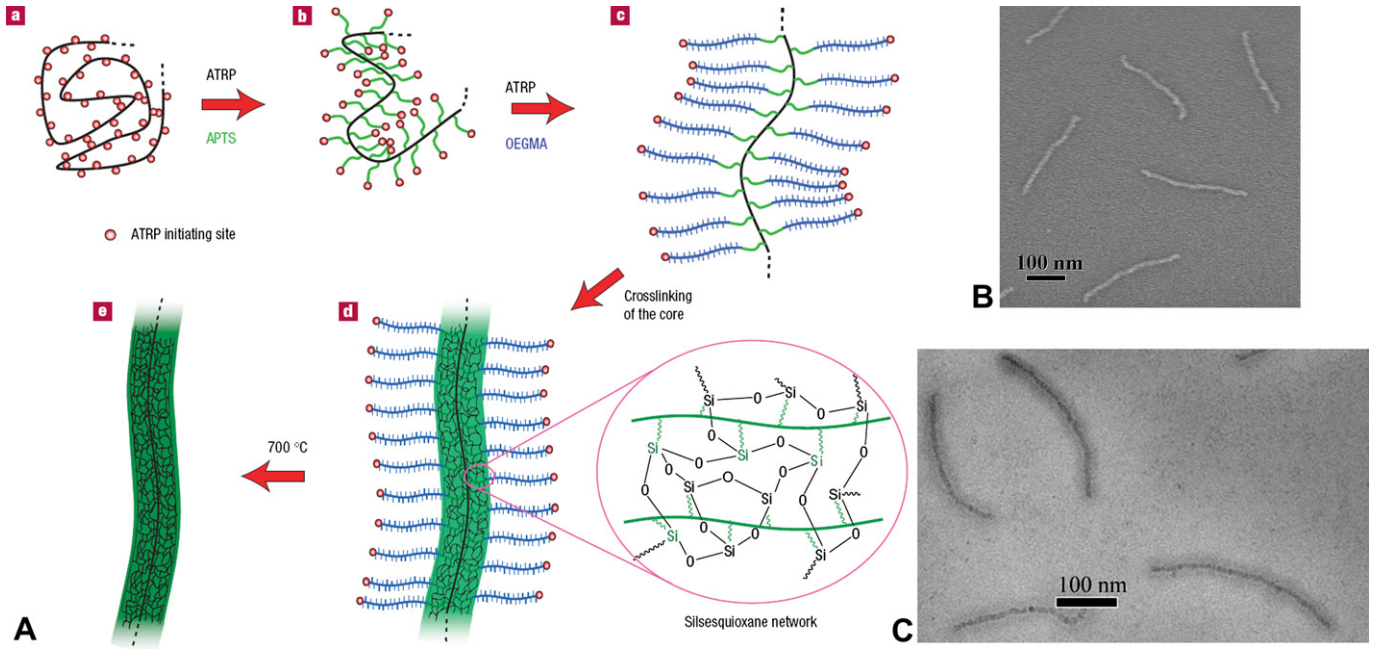

Fig. 11. (A) Synthesis of soluble organo-silica and inorganic silica nanowires: a ATRP polyinitiator (PBIEM) with degree of polymerization (DP) = 3200; b CPB with side chains of 20 APTS units; c core–shell CPB with an additional 57 OEGMA units; d soluble organo-silica hybrid nanowires with a crosslinked silsesquioxane network in the core; e inorganic silica nanowires after pyrolysis. (B, C) SEM and cryo-TEM (in water) images of organo-silica hybrid nanowires $[(SiO_{1.5})_{72}$-*b*-$OEGMA_{95}]_{3200}$, respectively [82]. Reprinted with the permission of Nature Publishing Group.

approach, a new "introducing into" strategy was developed to overcome these drawbacks, as shown in Fig. 12 [83]. A water-soluble bis-hydrophilic CPB with a poly(methacrylic acid) (PMAA) core and a POEGMA shell were first prepared. Presynthesized magnetite (Fe_3O_4) nanoparticles with an average diameter of 10 nm were mixed with brushes. It was found that the nanoparticles were introduced into the brush core. Excess nanoparticles were removed by ultrafiltration. A linear arrangement of the magnetite nanoparticles is clearly visible and agrees with the cylindrical morphology of the brushes. They were readily aligned when dried on a solid substrate in the presence of weak external magnetic fields (40–300 mT). This strategy provides a novel example of the alignment and directed assembly of polymer hybrid systems.

Morphologically, the CPBs are similar to cylindrical micelles self-assembled from surfactants or block copolymers in solution. Since the side chains are covalently bound to the main chain in CPBs, they exhibit a superior stability with regard to self-assembled cylinders against external stimuli such as temperature, solvent, and pH. In addition, their size distribution can be much easier controlled. However, it is difficult to exceed lengths of 1 μm.

3.1.3. *Biological superstructures*

Nature offers a multitude of organic nanostructures with unmatchable complexity and functionality. They control the mineralization and nanocrystal synthesis of various metals in exact shapes and sizes with high reproducibility and accuracy. In some natural biological nanostructures, the building blocks are combined preferentially into a 1D manner. Typical examples include cellulose [84,85], collagen [86,87], DNA [88–92], and viruses [93–100]. These originally elongated biologic nano-objects can be harvested directly from plants or animals for the localization and conversion of inorganic precursors to nanostructures on their interior or outer surfaces. Among them, DNA is the most frequently employed natural 1D template. Usually, coating DNA with metal nanoparticles, so-called metallization, has three sequential steps. The first step is the binding of metal ions or metal complexes to DNA strands to create reactive metal sites. This activation step is based on either exchanging ions with the DNA backbone or the insertion of metal complexes between the DNA bases. In the second step, the reactive metal sites are usually treated with a reducing agent. This converts the metal ions or metal complexes into metal nanoclusters attached to the DNA strand. The third step is the autocatalytic growth of these affixed metal nanoclusters, which are able to act as seeds because of the simultaneous presence of both metal ions/metal complexes and reducing agents in the growth solution. In this step, a second metal ion could be deposited on the DNA scaffold. For example, Co nanoparticles could grow on the Pt nanoseeds in the third step to form magnetic Co nanowires on the DNA instead of Pt nanowires (Fig. 13) [90].

The tobacco mosaic virus (TMV) is another natural template commonly used for the fabrication of 1D organic–inorganic

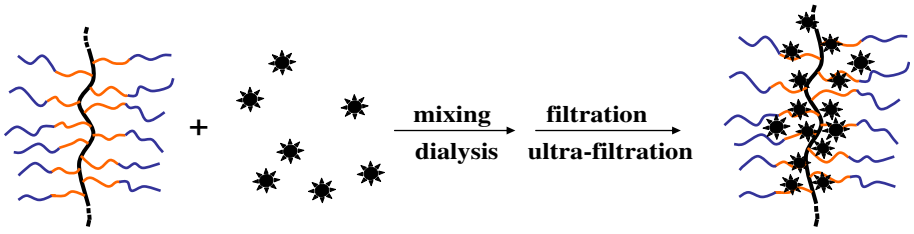

Fig. 12. Synthetic route to water-soluble superparamagnetic hybrid nanocylinders templated by core–shell cylindrical brushes via an "introducing into" strategy.

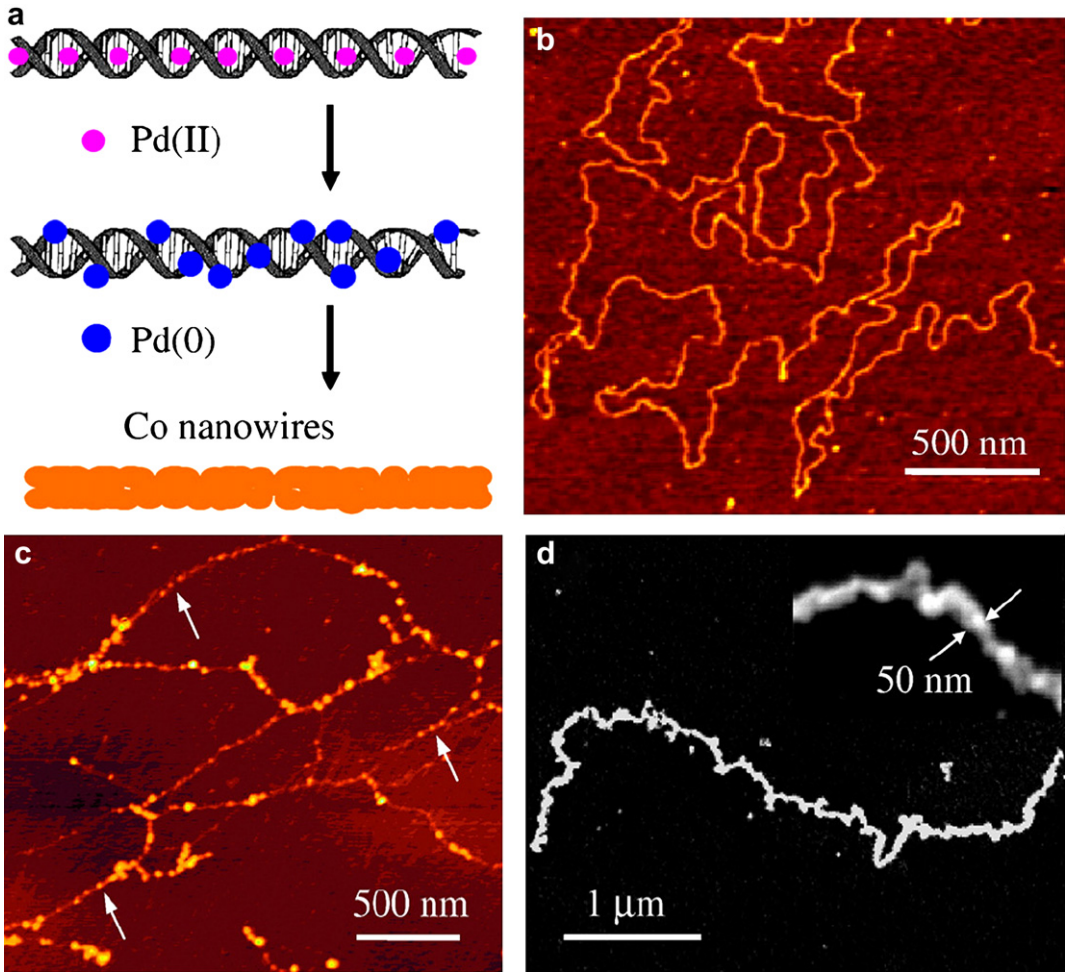

Fig. 13. (a) Illustration of Pd nanoparticle-seeded Co nanowire growth on DNA, (b) AFM height image of unmodified DNA molecules (z range: 1 nm), (c) AFM image of Pd seeds (1–3 nm) coated DNA (z range: 3.5 nm), and (d) SEM image of a single continuous Co nanowire (inset is the enlarged view) [90]. Reprinted with the permission of Elsevier.

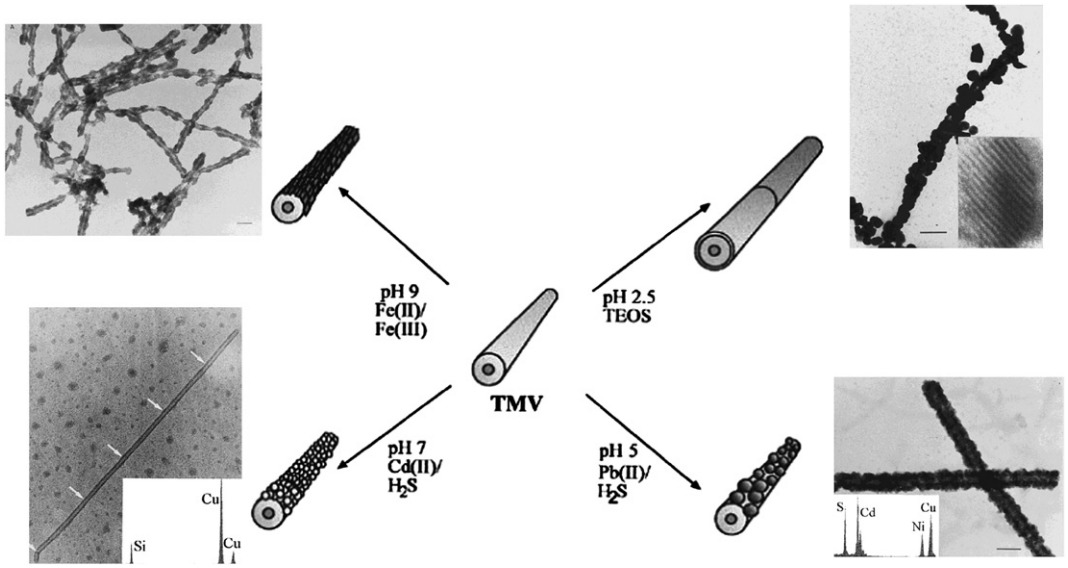

Fig. 14. Synthetic route to nanotube hybrids using TMV templates. Clockwise from top right: sol–gel condensation (silica); coprecipitation (PbS and CdS nanocrystals, respectively); oxidative hydrolysis (iron oxide) [100]. Reprinted with the permission of Wiley-VCH.

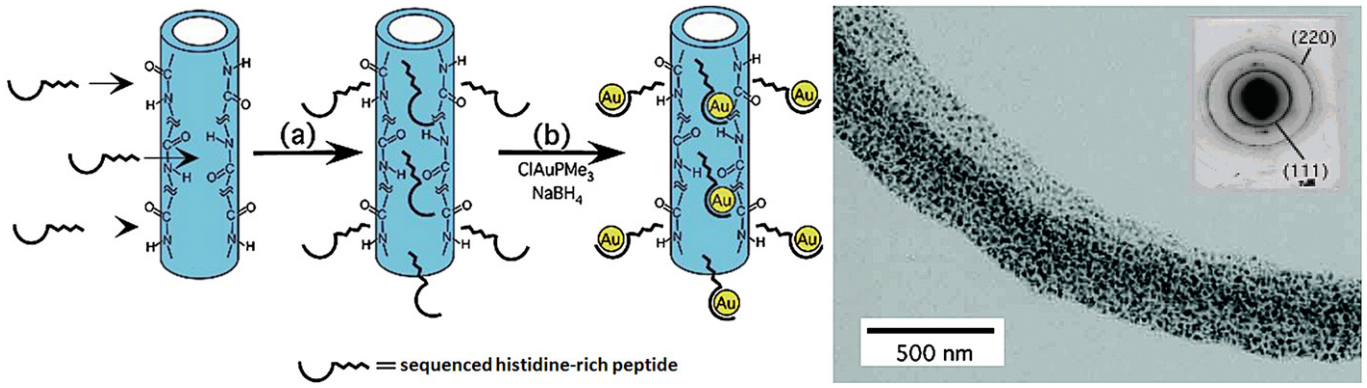

Fig. 15. Left: scheme of Au nanowire fabrication from peptide assemblies. (a) The immobilization of sequenced histidine-rich peptides at the amide-binding sites of the heptane dicarboxylate nanowires. (b) Au coating nucleated at the histidine sites of the nanowires. Right: TEM image of Au on the nanowire coated with the sequenced histidine-rich peptide (inset: electron diffraction of Au on the nanowire) [101]. Reprinted with the permission of ACS.

hybrids. The TMV is a remarkably stable virus, remaining intact at temperatures up to 60 °C and at pH values between 2 and 10. Each viral particle is 300 × 18 nm in size, with a 4 nm wide central channel. The internal and external surfaces consist of repeated patterns of charged amino acid residues, such as glutamate, aspartate, arginine, and lysine. Mann et al. demonstrated the versatility of the TMV as a template for the fabrication of a range of nanotubular organic–inorganic hybrids, as shown in Fig. 14 [100]. In the case of silica mineralization from acidic solutions (pH < 3), strong interactions are supposed to occur between the TMV particles and anionic silicate species formed by the hydrolysis of TEOS because of positive charges on the protein surface below the isoelectric point. By comparison, the preferential deposition of CdS, PbS, and iron oxides on the TMV external surface at mild pH conditions can be achieved by specific metal ion binding onto the numerous glutamate and aspartate surface groups.

Another example of applying biologically controlled mineralization is using sequenced peptide functionalized 1D objects as templates. For example, histidine-containing peptides show high affinities to metal ions. Although this complexation deforms proteins in organisms, it can be utilized to template the synthesis of metal nanocrystals. Matsui et al. reported that sequenced histidine-rich peptide molecules could self-assemble onto bis(*N*-α-amidoglycylglycine)-1,7-heptane dicarboxylate nanowires (Fig. 15) [101]. The biological recognition of the sequenced peptide selectively trapped $AuCl_4$ ions for the nucleation of Au nanocrystals. After the $AuCl_4$ ions had been reduced, highly monodispersed Au nanocrystals homogeneously covered the surface of the nanowires, producing peptide–Au hybrid nanowires [83].

3.1.4. Channels in porous materials

Channels in porous membranes provide another class of templates for the synthesis of 1D hybrid nanostructures. For this approach, the template contains very small cylindrical pores or voids within the host material. The empty spaces are filled with the chosen material, which adopts the pore morphology to form 1D nanostructured systems. Various types of porous materials, including commercially available porous polymeric membranes [102–104] and anodic aluminium oxide (AAO) films [75,105–109], have been used. Among them, alumina films are the most promising materials because of their regular channels with little or no tilting with respect to the surface normal. Furthermore, they exhibit a high pore density with a possible regular pattern. To create 1D hybrid nanomaterials, inorganic and organic components are simply introduced into the channels either simultaneously or sequentially to achieve the spatial organization of dissimilar and commonly incompatible components. When the inorganic and organic precursors are introduced and treated sequentially, core–shell- or block-type-structured 1D hybrid nanomaterials should be formed. For example, arrays of TiO_2 tubules were first synthesized within the pores of an alumina membrane via the sol–gel process. After the thermal treatment of the TiO_2 tubules, pyrrole was introduced into the inner core of TiO_2 nanotubes and conductive polypyrrole (PPy) nanowires were grown by polymerization (Fig. 16). The as-synthesized hybrid possesses a PPy core with an excellent electrical conductivity and a TiO_2 shell with photocatalytic activity and high surface area [102]. Employing the same strategy, more complicated structures such as conductor–insulator–conductor concentric carbon–polyacrylonitrile–gold tubules have been fabricated.

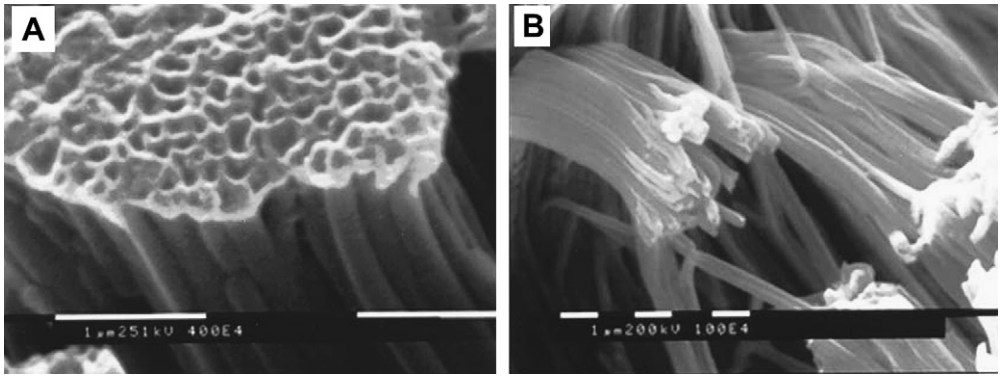

Fig. 16. SEM images of TiO_2 nanotubules prepared by sol–gel methods before (A) and after (B) filling with the polypyrrole nanowires. The outer diameter of the tubular composite is 200 nm [102]. Reprinted with the permission of RSC.

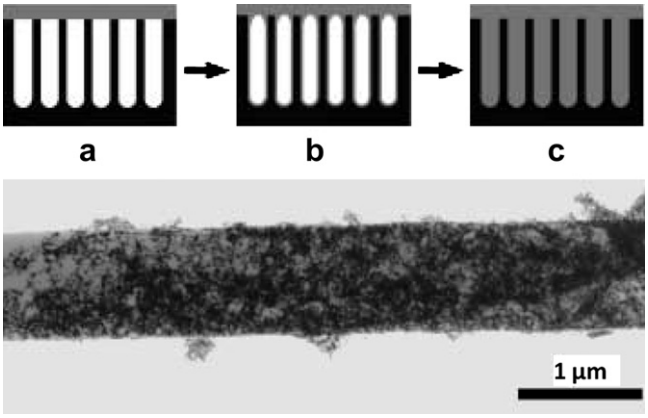

Fig. 17. Top: schematic representation of the different stages of pore wetting: a) a liquid containing a polymeric component on a pore array, b) wetting state, and c) complete filling. Bottom: TEM image of a tube with a core–shell morphology, which was prepared by consecutive wetting steps. The outer shell is a network of Pd, whereas the inner core consists of PS [111,113]. Reprinted with the permission of Wiley-VCH.

Using the same template, Greiner et al. developed a wetting-assisted templating (WASTE) process. Instead of completely filling the pores in the alumina template, they only wetted the walls inside the pores [110–115]. After removing the template, a nanotube is formed. This process is related to the special wetting phenomena of polymer-based melts or liquids on the pore walls of a nanoporous membrane. In the case of viscous liquid, caused by the entanglement of polymers, the wall wetting and complete filling take place on different timescales, which allows the possible vitrification of the wetting state by either cooling the polymer melt below its crystallization/glass transition temperature or, in the case of polymeric solutions, by evaporating a volatile solvent. Nanotubes with walls composed of a broad range of inorganic, organic, and hybrid materials are accessible. For example, polylactide (PLA)–Pd hybrid nanotubes have been prepared by such a method (Fig. 17) [111]. First, PLA with palladium acetate was mixed in dichloromethane (bp: 38 °C). The solution was used to wet the pores. Heating to a temperature of about 150 °C leads to a reduction of palladium acetate in the Pd nanoparticles. At a high temperature of 200 °C, the PLA polymer thermally degrades and a stable tubular

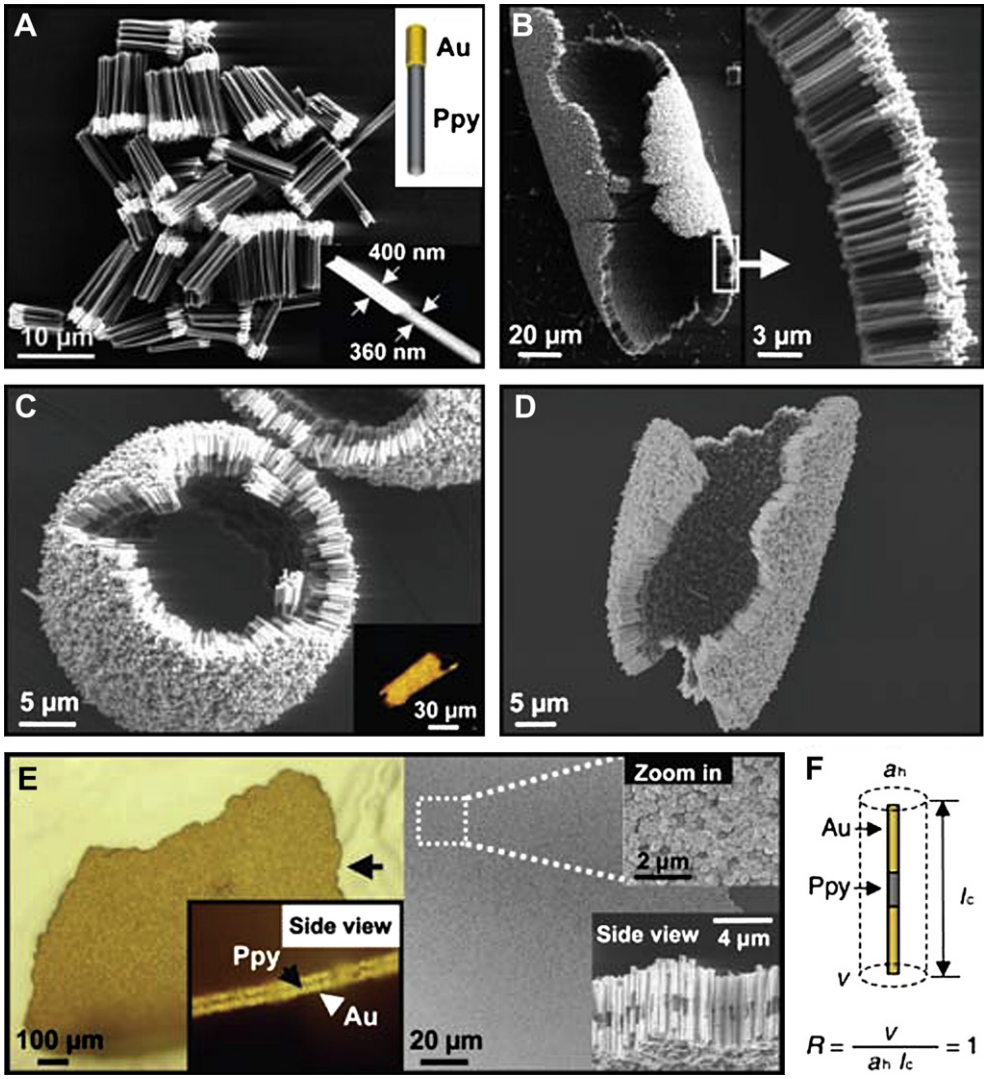

Fig. 18. (A) SEM images of the as-synthesized Au–PPy rods. (B–D) SEM images of the assemblies of Au–PPy rods with 1:4, 3:2, and 4:1 block length ratios, respectively. (E) (Left) Optical and (right) SEM images of a planar assembly of three-component rods (Au–PPy–Au), respectively. (F) A schematic representation of the Au–PPy-Au three-component rods [116]. Reprinted with the permission of AAAS.

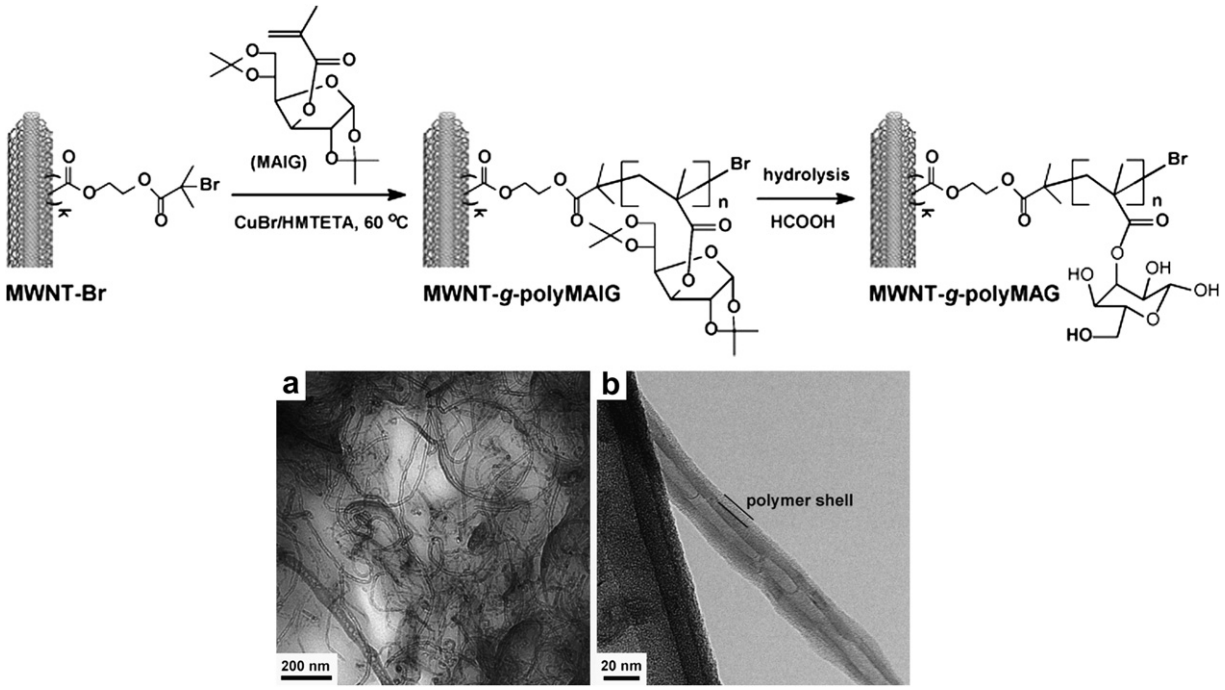

Fig. 19. Top: synthetic strategy for grafting a linear glycopolymer from surfaces of MWNTs by ATRP. Bottom: TEM images of linear glycopolymer-functionalized MWNTs at 29 (a) and 10.5 h (b) after the polymerization of MAIG from the CNT surface [126]. Reprinted with the permission of ACS.

porous Pd nanotube is formed, which can be filled with PS to render a hybrid nanotube with a core–shell PS–Pd morphology.

A unique 1D hybrid nanostructure consisting of segmented hard (inorganic) and soft (organic) domains has been accessed by using an AAO template (Fig. 18). The hard hydrophilic domain is an inorganic material such as gold and the soft domain is a hydrophobic-conducting polymer such as polypyrrole (PPy), which can be electrochemically polymerized within the channels of an alumina template [116]. As a result of the compositional differences between the inorganic and organic portions, the block ends tend to phase segregate in a way that would align the structures to maximize the interactions between blocks of similar composition, similar to an amphiphilic diblock copolymer but different with respect to size and the fact that one block is made of a rigid inorganic material. A flat 2D as well as a curved 3D superstructure was formed through the assembly of the metal–polymer-segmented rod-like hybrids with different ratios.

3.1.5. *Hybridizing existing 1D objects*

Currently existing inorganic, organic, or even hybrid 1D objects are immediately useful as templates. From an inorganic 1D nanostructure, a hybrid can be generated by simply introducing the organic or hybrid phase for a desired purpose. The formed hybrid 1D nanomaterials are considered either the final product or an intermediate of an inorganic or organic nanostructure. The most frequently reported morphology prepared from this method is the coaxial nanocable, namely coating the inorganic surface directly with conformal sheaths, mainly polymers [117–125].

A well-studied example is that of CNTs, which are one of the most fascinating 1D nano-objects with a wide range of applications. To explore and realize their potential, the functionalization of CNTs has been performed [126–132]. In this regard, many polymers have been grafted onto or from the convex surfaces of CNTs to prepare polymer-coated nanotubes. For example, sugar-containing biocompatible glycopolymers have been grafted from the surfaces

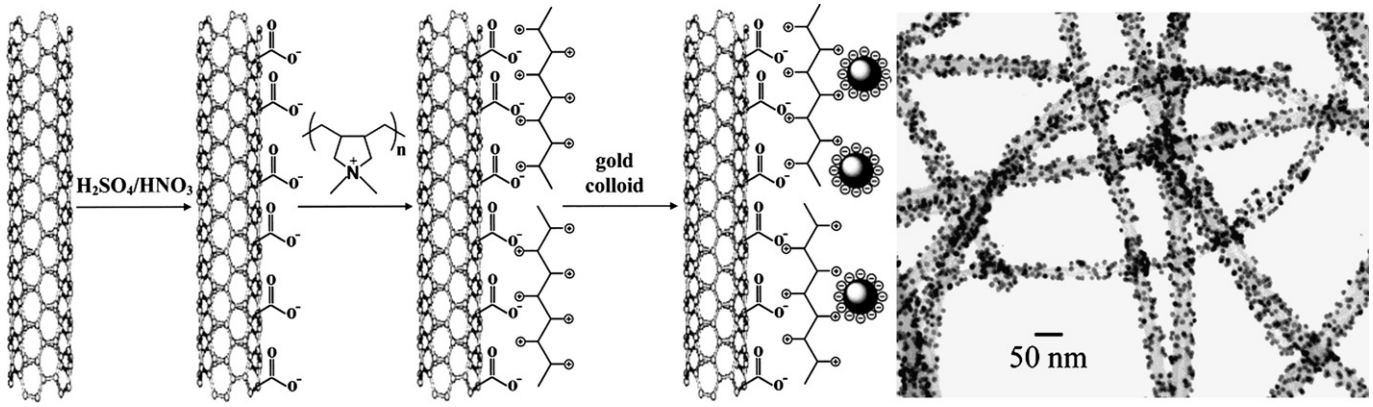

Fig. 20. Left: schematic view of the process for anchoring gold nanoparticles to nitrogen-doped CNTs. Right: TEM image of gold nanoparticle–CNTs hybrid structures [133]. Reprinted with the permission of ACS.

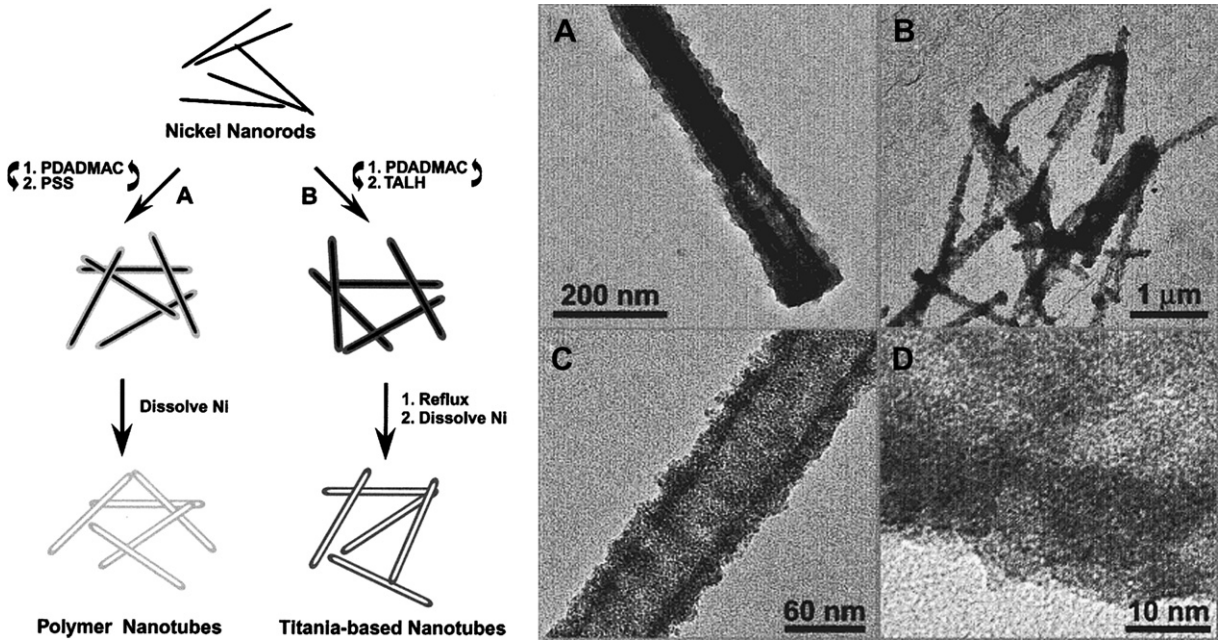

Fig. 21. Left: schematic illustration of the preparation of polymer and inorganic–organic composite nanotubes using the LbL-CT strategy. Right: TEM images of (A) a nickel nanorod coated with a titania/PDADMAC coating, (B) titania/PDADMAC nanotubes obtained on the dissolution of coated nickel nanorods, (C) a higher magnification image of a nanotube, and (D) a high-resolution image of a composite (titania/PDADMAC) nanotube showing the titania nanoparticles [134]. Reprinted with the permission of ACS.

of multi-wall carbon nanotubes (MWNTs). This process involves the immobilization of ATRP-initiating groups onto nanotubes surface, and the subsequent polymerization of 3-O-methacryloyl-1,2:5, 6-di-O-isopropylidene-D-glucofuranose (MAIG) from the surface (Fig. 19) [126]. The resulting multihydroxy glycopolymer-functionalized CNTs show improved stability in solution, which have potential applications in the fields of tissue engineering and bionanotechnology.

When necessary, the grafted polymeric layer on the CNTs can be further decorated with functional nanoparticles. For example, gold nanoparticles have been reported to selectively attach to chemically functionalized surface sites on nitrogen-doped CNTs (Fig. 20) [133]. In this example, a cationic polyelectrolyte was adsorbed on the surface of the nanotubes by electrostatic interaction between the carboxyl groups on the chemically oxidized nanotube surface and polyelectrolyte chains. Negatively charged Au nanoparticles from a gold colloid suspension were subsequently anchored to the surface of the nanotubes through the electrostatic interaction between the polyelectrolyte and the nanoparticles. This approach can be generalized to functionalize CNTs with various nanoparticles by using a polyelectrolyte as a linker.

Taking advantage of the layer-by-layer colloid-templating (LbL-CT) approach, Caruso and co-workers developed a versatile technique for the preparation of polymer–inorganic hybrid core–shell nanocables. As an example illustrated in Fig. 21, it is based on the electrostatic self-assembly of two oppositely charged polyelectrolytes poly (diallyldimethylammonium chloride) (PDADMAC) and poly(sodium 4-styrenesulfonate) (PSSNa) onto nickel nanorods [134]. Besides these oppositely charged polyelectrolytes, a combination of a polyelectrolyte and a titania precursor (titanium (IV) bis(ammonium lactato) dihydroxide) as the depositing partners, a hierarchical 1D hybrid with a nickel core, and a titania–polyelectrolyte hybrid shell is

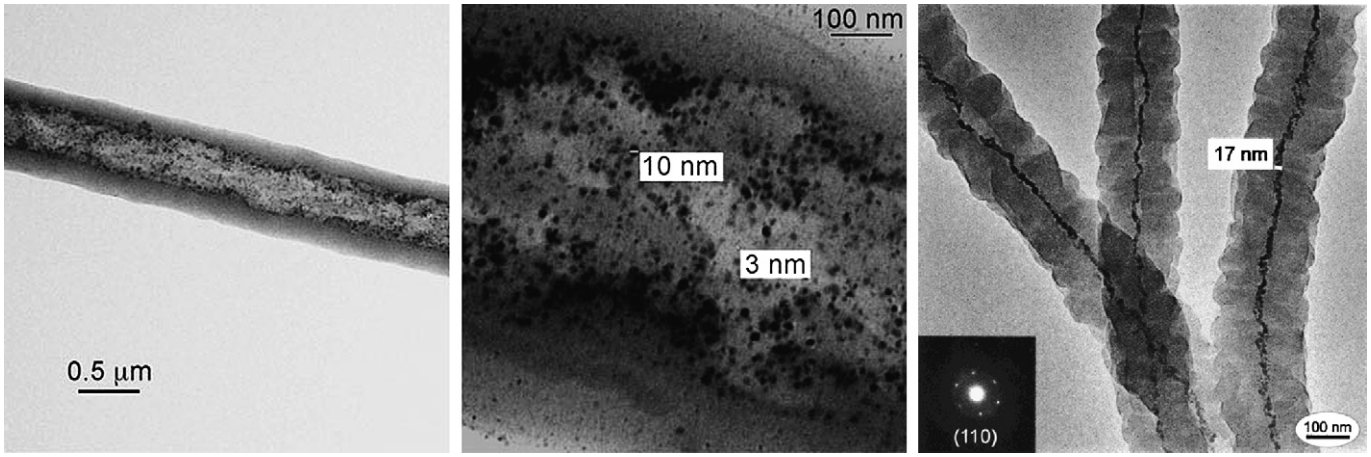

Fig. 22. TEM micrographs of different sized PPX nanotubes containing Pd nanoparticles in the inner core. The middle one is the enlarged view of the left [135,137]. Reprinted with the permission of Springer and ACS.

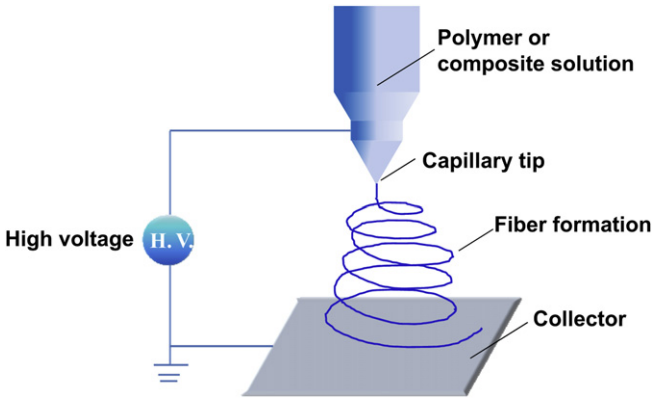

Fig. 23. Illustration of an electrospinning experiment.

formed as an intermediate. Removing the nickel rod as the core, a titania–polyelectrolyte hybrid nanotube is then prepared. As an apparent advantage of the layer-by-layer technique, the thickness of the polymeric layer in this method is simply controlled by the circles of polyelectrolyte deposition.

Besides templating with existing inorganic 1D objects, several groups have obtained coaxial nanocable structures and nanotubes from existing 1D polymeric or hybrid objects. A "tubes by fiber templates" (TUFT) process was used by Greiner et al. to prepare various hybrid nanotubes [135–140]. For example, poly(p-xylylene) (PPX) tubes loaded with metal nanoparticles such as Pd, Ag, or Cu in the inner core can be prepared by coating PLA/metal acetate hybrid nanofibers by PPX via a chemical vapor deposition process, followed by the conversion of metal acetate to metal nanoparticles and the degradation of PLA. The inner core of the tubular structure is controlled by the diameter of the original PLA/metal acetate hybrid nanofibers (Fig. 22). Similarly, coating polycarbonate fibers with a ZnO sheath and cellulose acetate fibers with polyoxometalate have also been reported [141,142].

3.2. Electrospinning techniques

Electrospinning has been actively explored as a highly versatile and simple method to process polymer-containing solutions or melts into continuous fibers with diameters ranging from micro- to nanometers. This method has gained substantial academic attention since the 1990s because of the close combination of both fundamental and application-oriented research including scientific and engineering disciplines. This technique involves the use of a high voltage to charge the surface of a polymer solution droplet and thereby induce the ejection of a liquid jet through a spinneret (Fig. 23). Owing to the bending instability, the jet is subsequently stretched many times to form continuous, ultrathin fibers. Currently, electrospinning is the only technique that allows the fabrication of continuous ultralong fibers with diameters down to a few nanometers. The method can be applied to virtually all soluble or fusible polymers, polymer alloys, and polymers loaded with various kinds of nanoparticles or active agents(Fig. 24). The scope of applications, in fields as diverse as optoelectronics, sensor technology, catalysis, filtration, and medicine, is very broad [143–145].

Several reports have described the electrospinning of hybrid nanofibers based on polymeric and inorganic moieties. Owing to the large number of suitable candidates in both fields, the combination of two ingredients results in a giant family of polymer–inorganic hybrid nanofibers. The incorporated inorganic components include salts, clay, CNTs, metal, metal oxide or chalcogenide nanoparticles. Electrospinning hybrid fibers containing montmorillonite with polyamide 6 [146–148], polyamide 6,6 and poly(vinyl acetate) (PVA) [149], poly(methyl methacrylate) (PMMA) [150], and polyurethane (PU) [151] as the carrier material have been described. CNTs can be immobilized in electrospun polymer fibers to improve electrical conductivity or mechanical strength. Examples of polymers that were spun with CNTs into the corresponding hybrid fibers include poly(acrylonitrile) (PAN), poly(ethylene oxide) (PEO), PVA, PLA, polycarbonate (PC), PS, PU, PMMA, polyaniline [152–158], and so forth. Examples of electrospinning polymer hybrid fibers containing noble metal nanoparticles include PAN/Ag [159,160], Nylon 6/(Ag, Au, Pt) [161], PAN-co-PAA/Pd [162],

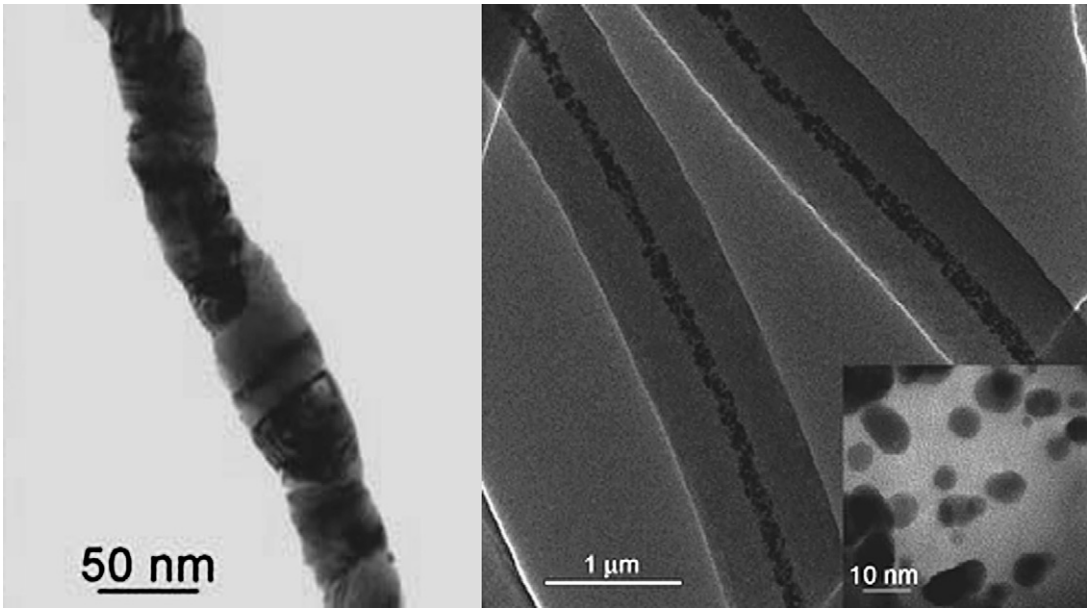

Fig. 24. Left: TEM image of a copper nanofiber obtained from electrospun poly(vinyl butyral) (PVB)/$CuNO_3$ composite fibers. Right: TEM image of nanofibers loaded with bimetallic nanoparticle catalysts [144]. Reprinted with the permission of Wiley-VCH.

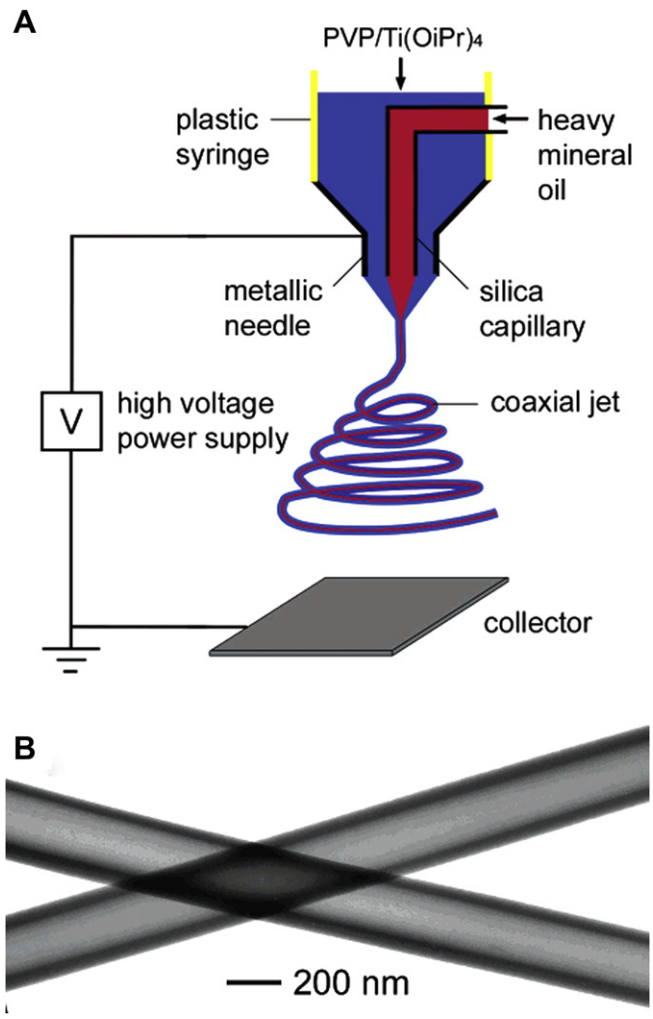

Fig. 25. (A) Illustration of the setup for electrospinning nanofibers with a core/sheath structure. (B) TEM image of two as-spun hollow fibers after the oily cores had been extracted with octane. The walls of these tubes are made of a composite containing amorphous TiO_2 and PVP [176]. Reprinted with the permission of ACS.

poly(vinylpyrrolidone) (PVP)/Ag [163], PEO/Ag [164], and others. Hybrid nanofibers loaded with monometallic or bimetallic nanoparticles (Fig. 24) are especially useful in the field of catalysis, for example, hydrogenation reactions. The immobilization of noble metal nanoparticles in nanofibers facilitates the removal and recycling of the catalysts after the reaction.

Combined with sol–gel processes, a variety of polymer–metal oxide (or metal chalcogenide) hybrid fibers have been produced by electrospinning, such as PVP/TiO_2 or PVP/ZrO_2 hybrids [165,166]. Further examples of metal oxides and chalcogenides that have been incorporated into polymer nanofibers are PbS [167], NiO [168], PVP/Fe_3O_4 [169], PPV/Fe_3O_4 [170], ZnO [171], CdS [172], CdSe [173], and so forth. Metal-containing salts [141] and nanodiamonds [142] have also been introduced into polymers by electrospinning.

The conventional setup for electrospinning using a single capillary as the spinneret is only suitable for generating solid fibers or particles with one particular composition in each run of fabrication. Recently, new setups have been demonstrated to broaden the application spectrum of electrospinning [174–177]. For example, electrospinning with a dual syringe system (in the side-by-side fashion) has been set to electrospin biocomponent nanofibers for the fabrication of solid fibers [174]. Recently, by electrospinning two immiscible liquids through a coaxial, two-capillary spinneret, followed by the selective removal of the cores, hollow nanofibers with walls made of inorganic–polymer hybrids or ceramics after calcination have been prepared [175–177]. Xia et al. demonstrated this concept by using heavy mineral oil for the core and an ethanol solution of PVP and $Ti(OiPr)_4$ as the materials for the sheath (Fig. 25). After the heavy mineral oil had been extracted with octane, TEM characterization clearly indicated the formation of tubular structures that are uniform in size and with an inner diameter and wall thickness of 200 and 50 nm, respectively. The tubular walls consist of amorphous TiO_2 and PVP. Using a PVP or PS solution for the core instead of mineral oil, a core–shell tubular hybrid titania structure was prepared.

3.3. 1D conjugation of nanoparticles

A directional organization process of nanoparticles into 1D nanomaterials is another way to create organic–inorganic hybrids. In this approach, hybrid or inorganic nanoparticles are first prepared and are then attached in a linear fashion, driven by a permanent/temporary dipole in each nanoparticle, by their amphiphilic nature or covalent bounds [178–182]. Thus, they resemble monomer units in a linear polymer chain. The advantage of such a liner attachment is that the diameter of the hybrid nanowire is chiefly determined by that of the nanoparticles. This facilitates the construction of hybrid nanowires with defined and ultrathin diameters down to a few nanometers from nanoparticles. For example, Pyun et al. described the synthesis and characterization of polymer-coated ferromagnetic cobalt nanoparticles [178]. The self-assembly of these dipolar magnetic nanoparticles was investigated in solutions cast onto supporting substrates, where the local nematic-like ordering of nanoparticle chains was observed along with a tendency of adjacent chains to form “zippering” configurations due to van der Waal’s interactions (Fig. 26).

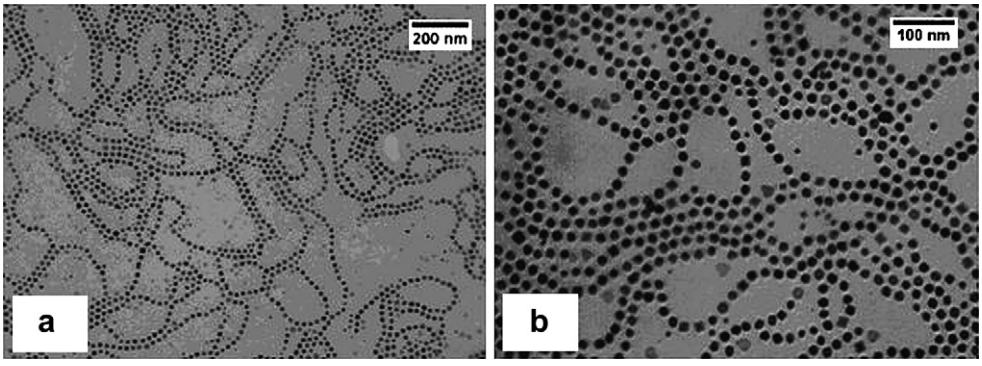

Fig. 26. TEM micrographs of PS–Co hybrid nanowires imaged at low (a) and high magnifications (b) [178]. Reprinted with the permission of ACS.

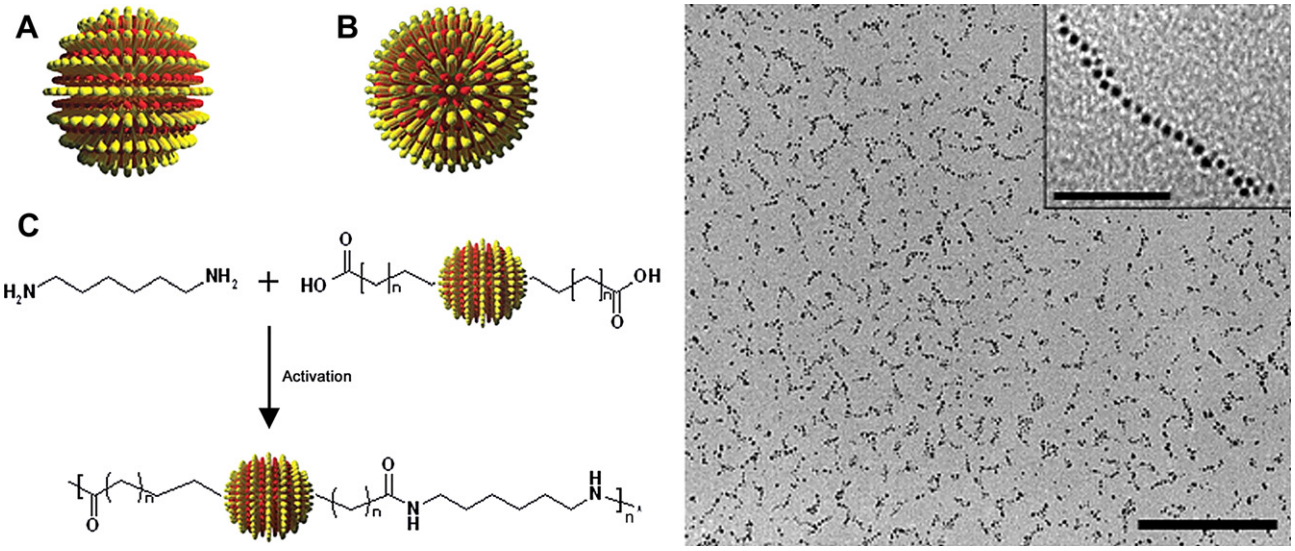

Fig. 27. Left: From rippled particles to nanoparticle chains. Idealized drawing of (A) a side view and (B) a top view of a rippled particle showing the two polar defects that must exist to allow the alternation of concentric rings. (C) Schematic depiction of the chain formation reaction. Right: TEM images of nanoparticles chains. Scale bars: 200 nm, inset: 50 nm [183]. Reprinted with the permission of AAAS.

The linear arrangement of nanoparticles through covalent bonds between adjacent nanoparticles has also been reported [183,184]. The obvious advantage of covalent bonding is the enhanced stability of the 1D hybrids against environmental changes. Ensuring the nanoparticles are connected linearly relies on the strict stoichiometric functionalization of nanoparticles. Stellacci et al. reported an approach to functionalize monolayer-protected gold nanoparticles at two diametrically opposed points that exist as a consequence of the topological nature of the particles. After the immobilization of two single carboxylic groups at both ends, they were employed as divalent building blocks ("artificial monomers") for a condensation reaction with complementary divalent molecules (1,6-hexanediamine as the "linker") to form chains (Fig. 27). The TEM image in Fig. 27 shows the as-synthesized linear string of gold nanoparticles. The interparticle distance here was determined to be 2.2 ± 0.4 nm. This spacing further increased to 4.2 ± 0.9 nm if *O,O′*-bis(2-aminoethyl)octadecaethylene glycol, a longer linker molecule, was used instead of 1,6-hexanediamine. Therefore, the interparticle spacing in the hybrid is tunable in terms of the linker molecules.

Besides spherical nanoparticles, nanorods can be considered building units for the oriented attachment. For example, gold nanorods were first synthesized in the presence of CTAB surfactants [180]. The two ends of the nanorods could be further tethered with thiol-terminated hydrophobic polystyrene chains to form ABA-type PS–Au–PS nanorod hybrid structures. The two polymeric phases at both ends of the inorganic nanorods act as "glue" to connect the gold nanorods end-to-end into extended linear, ring-like bundles as well as spherical hybrid superstructures in selective solvents (Fig. 28).

Apart from the 1D direct assembly of hybrid nanoparticles, another possibility by first assembling inorganic nanoparticles and then hybridizing the superstructure has also been demonstrated. In

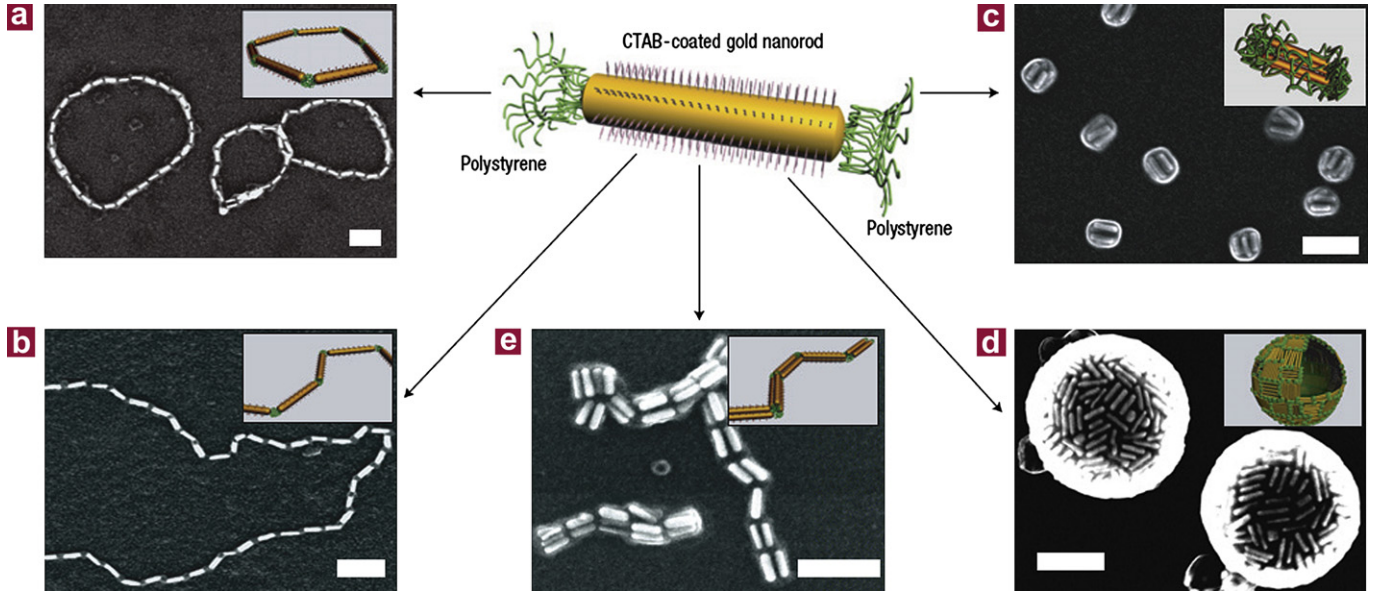

Fig. 28. Self-assembly of polymer-tethered gold nanorods into (a) rings, (b) chains, (c) bundles, (d) nanospheres, and (e) bundled nanorod chains [180]. Reprinted with the permission of Nature Publishing Group.

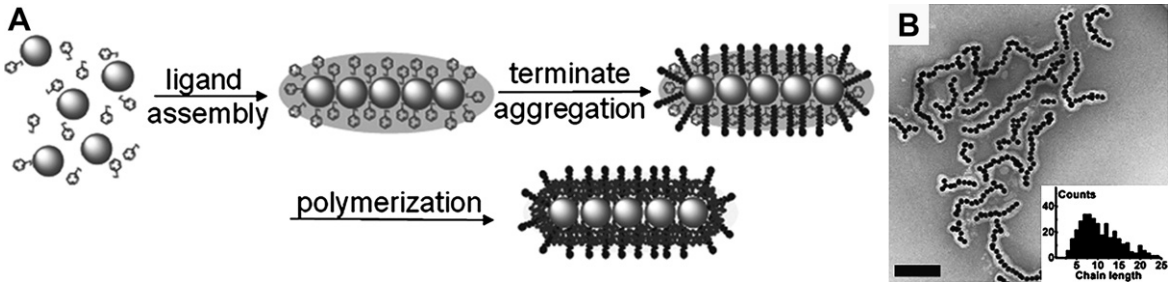

Fig. 29. Schematic illustration (A) and TEM image (B) of Au nanoparticles@PANI hybrid nanochains. Scale bar: 200 nm.[181]. Reprinted with the permission of RSC.

the process, the superstructure formed by the oriented attachment of inorganic nanoparticles acts as a dynamic 1D template, from which polymers are grafted to lock the anisotropic shape and simultaneously form the 1D hybrid nanostructure [26,181,182]. Chen et al. reported that in the presence of SDS the adsorption and *in situ* polymerization of aniline or pyrrole on the surface of gold nanoparticles gives uniform polymer shells (Fig. 29) [181]. By timing the SDS addition, nanochains formed through the linear aggregation of gold nanoparticles were fixed by the *in situ* formation of a conductive polymer shell, giving the Au-polypyrrole or Au-polyaniline (PANI) 1D hybrids that can be isolated (Fig. 27).

3.4. 1D hybrids prepared by other methods

1D organic–inorganic hybrid nanomaterials can be achieved by other synthetic approaches [29,185–196]. Since the organic phase is sensitive to high temperature (typically > 400 °C), these 1D hybrids were generated exclusively in the solution phase at mild heating conditions if required. The hybrids were formed by reacting the inorganic precursor with the organic phase in a controlled manner, leading to a structurally elongated morphology.

Sanchez et al. presented a general methodology for the designed synthesis of 1D organic–inorganic hybrid fibrous (fibers, rods, ribbons, helices, tubes, etc.) nanostructures templated through the use of organogelator-based supramolecular assemblies [197–199]. A broad family of silica, metal oxide, and non-oxide hybrid 1D nanostructures were prepared using this versatile method.

Xia et al. reported that a chain-like titanium glycolate complex, obtained from the reflux of $Ti(OR)_4$ (with R~–C_2H_5, -iso-C_3H_7, or -*n*-C_4H_9) in ethylene glycol at 170 °C, crystallized into uniform titanium glycolate hybrid nanowires [29]. Ti^{4+} is homogeneously distributed all over the 1D hybrid nanostructures at a molecular level, acting as the precursor of the porous titania nanowires that were obtained by calcination at 500 °C.

In a hydrothermal approach, a large amount of flexible silver/crosslinked PVA coaxial hybrid nanocables were fabricated in one step [185]. This approach makes use of the *in situ* reduction of $AgNO_3$ in the presence of PVA and the catalysis of silver ions on the crosslinking of PVA chains under hydrothermal conditions (Fig. 30, left). The formation of such elegant nanocables is controlled by a synergistic growth mechanism, named the synergistic soft/hard template mechanism. Here, PVA is responsible for both the formation of silver nanoparticles and the further oriented growth of silver nanowires stabilized by PVA; in turn, the silver wires act as a backbone on which crosslinked PVA will form. Similarly, Yu et al. reported an unusual necklace-like core–shell cable structure that formed by the hydrothermal treatment of a Cu precursor in a basic solution of PVA [186]. The necklace structure consists of a uniform Cu nanowire in its center and connected microbeads of crosslinked PVA along the nanowire (Fig. 30, right). The facile one-pot *in situ* solution approach has been applied for the preparation of other nanocable structures, such as Au-poly(3,4-ethylenedioxythiophene), Ag-polypyrrole, and tellurium-PVA [187–193].

In a different solution approach, unique helical hybrid silica bundles were obtained from a series of C_2-symmetric bridged silsesquioxanes synthesized from L- and D-valine [194,195]. The helical sense of the bundles can be controlled by changing the chirality of the silsesquioxanes, the carbon number of the central alkylene segments (an odd–even effect), and the polycondensation conditions. Moreover, hybrid silica nanotubes have recently been

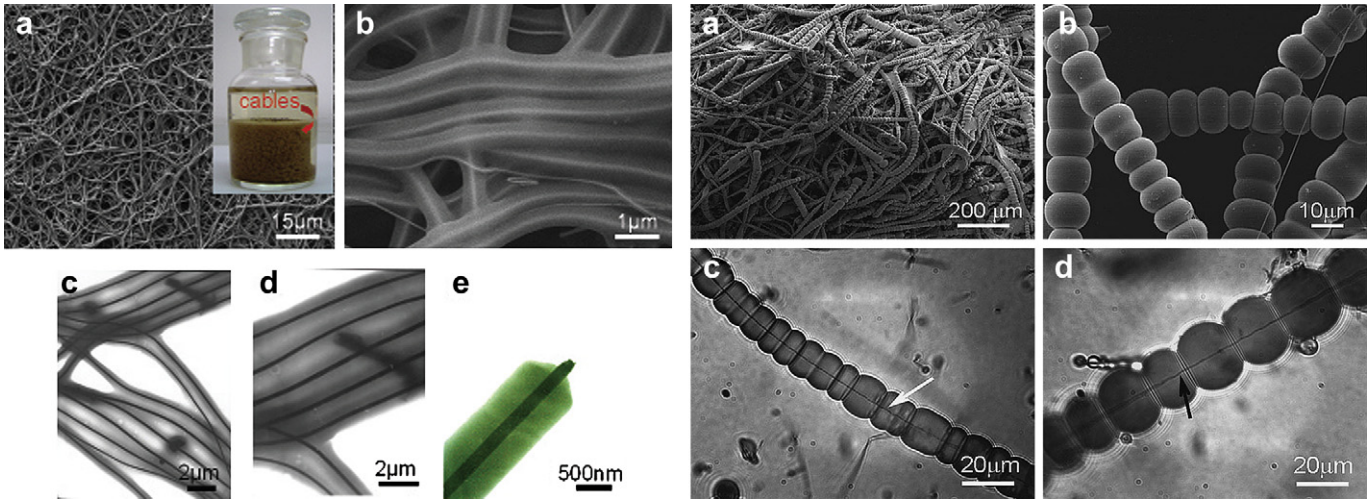

Fig. 30. Left: SEM (a, b) and TEM (c, d, e) images of Ag-PVA nanocables [185]. Right: SEM (a, b) and optical (c, d) images of the necklace-like microcables with different magnifications, showing the crosslinked PVA coatings on rather thin inner copper wire axes (indicated by arrows) [186]. Reprinted with the permission of ACS.

synthesized based on the non-equilibrium block copolymer self-assembly of poly(ethylene oxide)-*block*-poly(butylene oxide) [196]. The silica phase was introduced to trap the kinetically unstable tubules of the block copolymers.

1D hybrid nanostructures have also been formed by a ligand process in solution. The ligand, acting as a capping reagent, changes the free energies of the various crystallographic surfaces and thereby alters the growth kinetics of the facets of the crystals. As an example, uniform single crystalline tellurium (Te) nanorods have been synthesized in THF at room temperature using the poly(*tert*-butyl methacrylate) (P*t*BMA) polymer as the capping and oxidizing agent [200]. The P*t*BMA polymer chains are strongly bound to the circum-ambient crystal facets, and this promotes the preferential growth only along the (001) facet. This leads to the formation of Te nanorods with an aspect ratio as high as 21. Owing to the hybrid nature, namely with polymers firmly anchoring on their surface, these nanorods are fairly stable in THF, a good solvent for P*t*BMA. Although the polymer layer can be removed by thermal decomposition, it remained on the surface hybrid nanorods to enable the Te nanorods to assemble oleic acid-stabilized magnetite nanoparticles quantitatively on the surface in THF (Fig. 31). This specific behavior turns the semiconductor Te nanorods into magnetic nanocylinders, both of which show good stability in solution. The new function rendered by the magnetite nanoparticles on the nanorod surface makes it possible to align the Te nanorod-based magnetic nanocylinders on a solid substrate by depositing the nanocylinder solution in the presence of an external magnetic field [201]. An acid etching process was followed to dissolve the magnetite nanoparticles, leaving tellurium nanorods on the

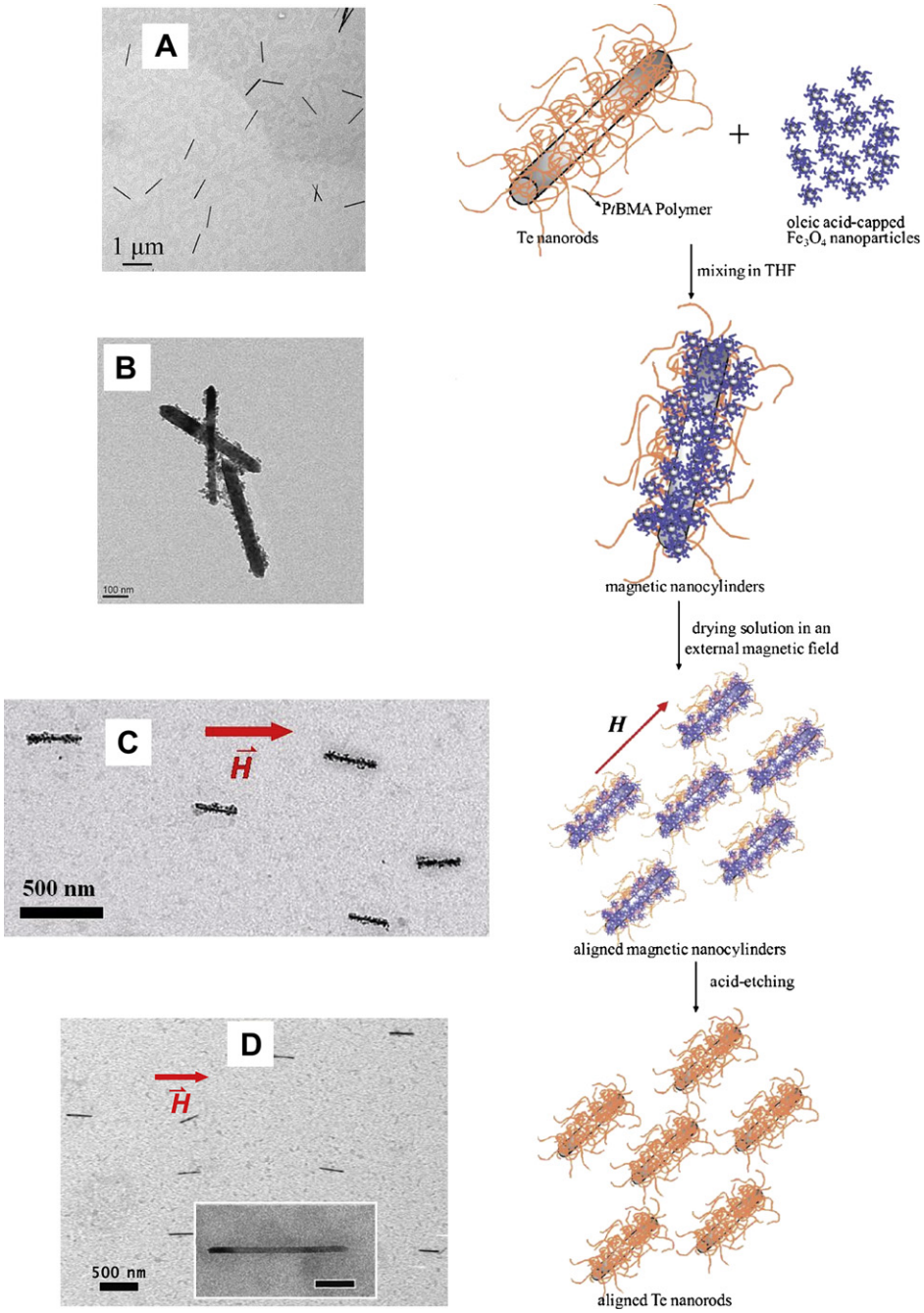

Fig. 31. Alignment of Te nanorods via the MAD process, assisted by an external magnetic field. (A–D) TEM images of Te nanorods, Te nanorods decorated with Fe_3O_4 nanoparticles, aligned magnetic nanocylinders, and aligned Te nanorods after etching away the magnetite nanoparticles, respectively [200,201]. Reprinted with the permission of Wiley-VCH and ACS.

substrate. This magnetization alignment demagnetization (MAD) process assisted by an external magnetic field is very useful to align non-magnetic 1D inorganic objects by hybridizing their surfaces with polymers [165–169].

4. Concluding remarks and perspectives

We have presented a brief review of recent work on 1D organic–inorganic hybrid nanomaterials based on the research activities in our group as well as in others. We first justified the interest in 1D organic–inorganic hybrid nanomaterials and then introduced the strategies for the construction of these nanostructures with various structures and architectures. As the major and robust methods, we detailed the state-of-the-art approaches of template-directed synthesis and the electrospinning technique. Currently, 1D nanomaterials based on organic and inorganic compounds remain in the focus of materials science. In the future, several directions deserve to be paid special attention. First, developing new synthetic methods of 1D organic–inorganic hybrid nanomaterials with desired morphologies and structures remains a key task. This can take advantage of and combine the latest proceedings in the fields of soft matter (colloids, polymers, biomacromolecules, etc.), hybrids, and inorganic materials. Second, a deep understanding of the organic–inorganic interface at the nanoscale, the collective behavior, and interparticle coupling among the 1D hybrids is crucial in nanoscience and nanotechnology. More effort is required to achieve the quantitative control of interfacial interactions. The theoretical modeling and prediction of 1D inorganic nanostructures has been a recent active research area; however, little attention is paid to that of 1D hybrids. Third, efficient and easy-to-implement methods are favored for organizing and manipulating 1D hybrid nanostructures at the mesoscale, as required for scientific and technological advances in their application in functional nanodevices. To date, only limited processes or techniques have been developed in this field, which have retarded the practical application of 1D hybrid nanostructures. Thus, the ability to assemble them into ordered and sometimes complex architectures is another challenge in this field.

References

[1] Burda C, Chen X, Narayanan R, El-Sayed MA. Chem Rev 2005;105:1025–102.
[2] Graetzel M. Nature 2001;414:338–44.
[3] O'Regan B, Graetzel M. Nature 1991;353:737–40.
[4] Wang X, Song J, Liu J, Wang ZL. Science 2007;316:102–5.
[5] Lee YJ, Yi H, Kim W-J, Kang K, Yun DS, Strano MS, et al. Science 2009;324:1051–5.
[6] Arico AS, Bruce P, Scrosati B, Tarascon J-M, van Schalkwijk W. Nat Mater 2005;4:366–77.
[7] Bruce PG, Scrosati B, Tarascon J-M. Angew Chem. Int Ed 2008;47:2930–46.
[8] Jaworowicz J, Vernier N, Ferre J, Maziewski A, Stanescu D, Ravelosona D, et al. Nanotechnology 2009;20. 215401/215401–215401/215404.
[9] Parkin SSP, Hayashi M, Thomas L. Science 2008;320:190–4.
[10] Beach GSD, Nistor C, Knutson C, Tsoi M, Erskine JL. Nat Mater 2005;4:741–4.
[11] Hayashi M, Thomas L, Moriya R, Rettner C, Parkin SSP. Science 2008;320:209–11.
[12] Bottero J-Y, Rose J, Wiesner MR. Integr Environ Assess Manage 2006;2:391–5.
[13] Li Q, Mahendra S, Lyon DY, Brunet L, Liga MV, Li D, et al. Water Res 2008;42:4591–602.
[14] Savage N, Diallo MS. J Nanopart Res 2005;7:331–42.
[15] Baccile N, Laurent G, Babonneau F, Fayon F, Titirici M-M, Antonietti M. J Phys Chem C 2009;113:9644–54.
[16] Titirici MM, Thomas A, Yu S-H, Müller J-O, Antonietti M. Chem Mater 2007;19:4205–12.
[17] Titirici M-M, Thomas A, Antonietti M. New J Chem 2007;31:787–9.
[18] Titirici M-M, Antonietti M, Baccile N. Green Chem 2008;10:1204–12.
[19] Xia Y, Yang P, Sun Y, Wu Y, Mayers B, Gates B, et al. Adv Mater 2003;15:353–89.
[20] Cademartiri L, Ozin GA. Adv Mater 2009;21:1013–20.
[21] Rao CNR, Deepak FL, Gundiah G, Govindaraj A. Prog Solid State Chem 2003;31:5–147.
[22] Law M, Goldberger J, Yang P. Annu Rev Mater Res 2004;34:83–122.
[23] Zhao YS, Fu H, Peng A, Ma Y, Xiao D, Yao J. Adv Mater 2008;20:2859–76.
[24] Hu J, Odom TW, Lieber CM. Acc Chem Res 1999;32:435–45.
[25] Liu Y, Ma Z, Ramakrishna S. Curr Nanosci 2006;2:71–8.
[26] Tang Z, Kotov NA. Adv Mater 2005;17:951–62.
[27] Law M, Sirbuly DJ, Johnson JC, Goldberger J, Saykally RJ, Yang P. Science 2004;305:1269–73.
[28] Johnson JC, Choi H-J, Knutsen KP, Schaller RD, Yang P, Saykally RJ. Nat Mater 2002;1:106–10.
[29] Jiang X, Wang Y, Herricks T, Xia Y. J Mater Chem 2004;14:695–703.
[30] Iijima S. Nature 1991;354:56–8.
[31] Kresge CT, Leonowicz ME, Roth WJ, Vartuli JC, Beck JS. Nature 1992;359:710–2.
[32] Murphy CJ, Jana NR. Adv Mater 2002;14:80–2.
[33] Jana NR, Gearheart L, Murphy CJ. Adv Mater 2001;13:1389–93.
[34] Mandal S, Müller AHE. Mater Chem Phys 2008;111:438–43.
[35] Spatz JP, Moessmer S, Möller M. Chem.–Eur J 1996;2:1552–5.
[36] Selvan ST, Spatz JP, Klok HA, Möller M. Adv Mater 1998;10:132–4.
[37] Spatz JP, Roescher A, Möller M. Adv Mater 1996;8:337–40.
[38] Duxin N, Liu F, Vali H, Eisenberg A. J Am Chem Soc 2005;127:10063–9.
[39] Massey JA, Temple K, Cao L, Rharbi Y, Raez J, Winnik MA, et al. Am Chem Soc 2000;122:11577–84.
[40] Raez J, Manners I, Winnik MA. J Am Chem Soc 2002;124:10381–95.
[41] Cao L, Manners I, Winnik MA. Macromolecules 2002;35:8258–60.
[42] Wang X-S, Winnik MA, Manners I. Angew Chem. Int Ed 2004;43:3703–7.
[43] Wang X, Guerin G, Wang H, Wang Y, Manners I, Winnik MA. Science 2007;317:644–7.
[44] Wang X, Wang H, Frankowski DJ, Lam PG, Welch PM, Winnik MA, et al. Adv Mater 2007;19:2279–85.
[45] Manners I. Angew Chem. Int Ed 2007;46:1565–8.
[46] Wang H, Winnik MA, Manners I. Macromolecules 2007;40:3784–9.
[47] Wang X, Liu K, Arsenault AC, Rider DA, Ozin GA, Winnik MA, et al. J Am Chem Soc 2007;129:5630–9.
[48] Wang H, Lin W, Fritz KP, Scholes GD, Winnik MA, Manners I. J Am Chem Soc 2007;129:12924–5.
[49] Guerin G, Wang H, Manners I, Winnik MA. J Am Chem Soc 2008;130:14763–71.
[50] Wang H, Wang X, Winnik MA, Manners I. J Am Chem Soc 2008;130:12921–30.
[51] Wang Y, Zou S, Kim KT, Manners I, Winnik MA. Chem.–Eur J 2008;14:8624–31.
[52] Li JK, Zou S, Rider DA, Manners I, Walker GC. Adv Mater 2008;20:1989–93.
[53] Shen L, Wang H, Guerin G, Wu C, Manners I, Winnik MA. Macromolecules 2008;41:4380–9.
[54] Rider DA, Manners I. Polym Rev 2007;47:165–95.
[55] Liu K, Fournier-Bidoz S, Ozin GA, Manners I. Chem Mater 2009;21:1781–3.
[56] Wang H, Patil AJ, Liu K, Petrov S, Mann S, Winnik MA, et al. Adv Mater 2009;21:1805–8.
[57] Gaedt T, Ieong NS, Cambridge G, Winnik MA, Manners I. Nat Mater 2009;8:144–50.
[58] Kaestle G, Boyen H-g, Weigl F, Lengl G, Herzog T, Ziemann P, et al. Adv Funct Mater 2003;13:853–61.
[59] Glass R, Arnold M, Bluemmel J, Kueller A, Möller M, Spatz JP. Adv Funct Mater 2003;13:569–75.
[60] Glass R, Möller M, Spatz JP. Nanotechnology 2003;14:1153–60.
[61] Spatz JP, Moessmer S, Hartmann C, Möller M, Herzog T, Krieger M, et al. Langmuir 2000;16:407–15.
[62] Spatz JP, Eibeck P, Moessmer S, Möller M, Herzog T, Ziemann P. Adv Mater 1998;10:849–52.
[63] Park S, Kim B, Cirpan A, Russell TP. Small 2009;5:1343–8.
[64] Nagarajan S, Li M, Pai RA, Bosworth JK, Busch P, Smilgies D-M, et al. Adv Mater 2008;20:246–51.
[65] Nagarajan S, Russell TP, Watkins JJ. Adv Funct Mater 2009;19:2728–34.
[66] Park S, Wang J-Y, Kim B, Russell TP. Nano Lett 2008;8:1667–72.
[67] Park S, Kim B, Wang J-Y, Russell TP. Adv Mater 2008;20:681–5.
[68] Mendoza C, Gindy N, Gutmann JS, Fromsdorf A, Forster S, Fahmi A. Langmuir 2009;25:9571–8.
[69] Mendoza C, Pietsch T, Gutmann JS, Jehnichen D, Gindy N, Fahmi A. Macromolecules 2009;42:1203–11.
[70] Yan X, Liu G, Liu F, Tang BZ, Peng H, Pakhomov AB, et al. Angew Chem. Int Ed 2001;40:3593–6.
[71] Yan X, Liu G, Li ZJ. Am Chem Soc 2004;126:10059–66.
[72] Yan X, Liu G, Haeussler M, Tang BZ. Chem Mater 2005;17:6053–9.
[73] Yelamanchili RS, Walther A, Müller AHE, Breu J. Chem Commun; 2008:489–91.
[74] Walther A, Yuan J, Abetz V, Müller AHE. Nano Lett 2009;9:2026–30.
[75] Steinhart M. Adv Polym Sci 2008;220:123–87.
[76] Zhang M, Müller AHE. J Polym Sci. Part A Polym Chem 2005;43:3461–81.
[77] Djalali R, Li S-Y, Schmidt M. Macromolecules 2002;35:4282–8.
[78] Zhang M, Estournes C, Bietsch W, Müller AHE. Adv Funct Mater 2004;14:871–82.
[79] Zhang M, Drechsler M, Müller AHE. Chem Mater 2004;16:537–43.
[80] Yuan J, Drechsler M, Xu Y, Zhang M, Müller AHE. Polymer 2008;49:1547–54.
[81] Yuan J, Lu Y, Schacher F, Lunkenbein T, Weiss S, Schmalz H, et al. Chem Mater 2009;21:4146–54.
[82] Yuan J, Xu Y, Walther A, Bolisetty S, Schumacher M, Schmalz H, et al. Nat Mater 2008;7:718–22.
[83] Xu Y, Yuan J, Fang B, Drechsler M, Müllner M, Bolisetty S, et al. Adv Funct Mater 2010, accepetd for publication.
[84] Venkataramanan NS, Matsui K, Kawanami H, Ikushima Y. Green Chem 2007;9:18–9.
[85] Zollfrank C, Scheel H, Greil P. Adv Mater 2007;19:984–7.

[86] Bai H, Xu K, Xu Y, Matsui H. Angew Chem. Int Ed 2007;46:3319–22.
[87] Gottlieb D, Morin SA, Jin S, Raines RT. J Mater Chem 2008;18:3865–70.
[88] Richter J, Mertig M, Pompe W, Monch I, Schackert HK. Appl Phys Lett 2001; 78:536–8.
[89] Kundu S, Liang H. Adv Mater 2008;20:826–31.
[90] Gu Q, Haynie DT. Mater Lett 2008;62:3047–50.
[91] Nguyen K, Monteverde M, Filoramo A, Goux-Capes L, Lyonnais S, Jegou P, et al. Adv Mater 2008;20:1099–104.
[92] Kodama T, Jain A, Goodson KE. Nano Lett 2009;9:2005–9.
[93] Mao C, Solis DJ, Reiss BD, Kottmann ST, Sweeney RY, Hayhurst A, et al. Science 2004;303:213–7.
[94] Nam KT, Kim D-W, Yoo PJ, Chiang C-Y, Meethong N, Hammond PT, et al. Science 2008;322:44.
[95] Dujardin E, Peet C, Stubbs G, Culver JN, Mann S. Nano Lett 2003;3:413–7.
[96] Liu WL, Alim K, Balandin AA, Mathews DM, Dodds JA. Appl Phys Lett 2005;86. 253108/253101–253108/253103.
[97] Knez M, Sumser M, Bittner AM, Wege C, Jeske H, Martin TP, et al. Adv Funct Mater 2004;14:116–24.
[98] Knez M, Kadri A, Wege C, Gösele U, Jeske H, Nielsch K. Nano Lett 2006;6: 1172–7.
[99] Fonoberov VA, Balandin AA. Nano Lett 2005;5:1920–3.
[100] Shenton W, Douglas T, Young M, Stubbs G, Mann S. Adv Mater 1999; 11:253–6.
[101] Djalali R, Chen Y-f, Matsui H. J Am Chem Soc 2002;124:13660–1.
[102] Hulteen JC, Martin CR. J Mater Chem 1997;7:1075–87.
[103] Martin CR. Acc Chem Res 1995;28:61–8.
[104] Martin CR. Science 1994;266:1961–6.
[105] Schwirn K, Lee W, Hillebrand R, Steinhart M, Nielsch K, Gösele U. ACS Nano 2008;2:302–10.
[106] Lee W, Schwirn K, Steinhart M, Pippel E, Scholz R, Gösele U. Nat Nanotechnol 2008;3:234–9.
[107] Wang Y, Gösele U, Steinhart M. Chem Mater 2008;20:379–81.
[108] Wang Y, Gösele U, Steinhart M. Nano Lett 2008;8:3548–53.
[109] Wang Y, Qin Y, Berger A, Yau E, He C, Zhang L, et al. Adv Mater 2009; 21:2763–6.
[110] Dersch R, Steinhart M, Boudriot U, Greiner A, Wendorff JH. Polym Adv Technol 2005;16:276–82.
[111] Steinhart M, Wendorff JH, Wehrspohn RB. ChemPhysChem 2003;4:1171–6.
[112] Kriha O, Zhao L, Pippel E, Gösele U, Wehrspohn RB, Wendorff JH, et al. Adv Funct Mater 2007;17:1327–32.
[113] Steinhart M, Wehrspohn RB, Gösele U, Wendorff JH. Angew Chem. Int Ed 2004;43:1334–44.
[114] Steinhart M, Jia Z, Schaper AK, Wehrspohn RB, Gösele U, Wendorff JH. Adv Mater 2003;15:706–9.
[115] Richter S, Steinhart M, Hofmeister H, Zacharias M, Gösele U, Gaponik N, et al. Appl Phys Lett 2005;87. 142107/142101–142107/142103.
[116] Park S, Lim J-H, Chung S-W, Mirkin CA. Science 2004;303:348–51.
[117] Cheng Q, Pavlinek V, He Y, Li C, Saha P. Colloid Polym Sci 2009;287:435–41.
[118] Bishnu PK, Eugene RZ. Angew Chem. Int Ed 2009;121:7020–3.
[119] Lu X, Zhao Q, Liu X, Wang D, Zhang W, Wang C, et al. Macromol Rapid Commun 2006;27:430–4.
[120] Ye Q, Wang X, Hu H, Wang D, Li S, Zhou FJ. Phys Chem C 2009;113:7677–83.
[121] Chen A, Xie H, Wang H, Li H, Li X. Synth Met 2006;156:346–50.
[122] Wu W-T, Wang Y, Shi L, Zhu Q, Pang W, Xu G, et al. Nanotechnology 2005; 16:3017–22.
[123] Luo L-B, Yu S-H, Qian H-S, Gong J- Y. Chem–Eur J 2006;12:3320–4.
[124] Wei Q, Zhou W, Ji J, Shen J. Nanoscale Res Lett 2009;4:84–9.
[125] Obare SO, Jana NR, Murphy CJ. Nano Lett 2001;1:601–3.
[126] Gao C, Muthukrishnan S, Li W, Yuan J, Xu Y, Müller AHE. Macromolecules 2007;40:1803–15.
[127] Capek I. Adv Colloid Interface Sci 2009;150:63–89.
[128] Qin S, Qin D, Ford WT, Zhang Y, Kotov NA. Chem Mater 2005;17:2131–5.
[129] Petrov P, Stassin F, Pagnoulle C, Jerome R. Chem Commun; 2003:2904–5.
[130] Lou X, Detrembleur C, Pagnoulle C, Jerome R, Bocharova V, Kiriy A, et al. Adv Mater 2004;16:2123–7.
[131] Huang H-M, Liu IC, Chang C-Y, Tsai H-C, Hsu C-H, Tsiang RC- C. J Polym Sci. Part A Polym Chem 2004;42:5802–10.
[132] Shaffer MSP, Koziol K. Chem Commun; 2002:2074–5.
[133] Jiang K, Eitan A, Schadler LS, Ajayan PM, Siegel RW, Grobert N, et al. Nano Lett 2003;3:275–7.
[134] Mayya KS, Gittins DI, Dibaj AM, Caruso F. Nano Lett 2001;1:727–30.
[135] Sun Z, Zeng J, Hou H, Wickel H, Wendorff JH, Greiner A. Prog Colloid Polym Sci 2005;130:15–9.
[136] Bognitzki M, Hou H, Ishaque M, Frese T, Hellwig M, Schwarte C, et al. Adv Mater 2000;12:637–40.
[137] Hou H, Jun Z, Reuning A, Schaper A, Wendorff JH, Greiner A. Macromolecules 2002;35:2429–31.
[138] Ochanda F, Jones Jr WE. Langmuir 2005;21:10791–6.
[139] Caruso RA, Schattka JH, Greiner A. Adv Mater 2001;13:1577–9.
[140] Ochanda F, Cho K, Andala D, Keane TC, Atkinson A, Jones WE. Langmuir 2009;25:7547–52.
[141] Ji L, Medford AJ, Zhang X. Polymer 2009;50:605–12.
[142] Behler KD, Stravato A, Mochalin V, Korneva G, Yushin G, Gogotsi Y. ACS Nano 2009;3:363–9.
[143] Agarwal S, Wendorff JH, Greiner A. Polymer 2008;49:5603–21.
[144] Greiner A, Wendorff JH. Angew Chem. Int Ed 2007;46:5670–703.
[145] Li D, Xia Y. Adv Mater 2004;16:1151–70.
[146] Fong H, Liu W, Wang C-S, Vaia RA. Polymer 2001;43:775–80.
[147] Cai Y, Li Q, Wei Q, Wu Y, Song L, Hu YJ. Mater Sci 2008;43:6132–8.
[148] Li Q, Wei Q, Wu N, Cai Y, Gao WJ. Appl Polym Sci 2008;107:3535–40.
[149] Ristolainen N, Heikkila P, Harlin A, Seppala J. Macromol Mater Eng 2006;291: 114–22.
[150] Kim G-M, Lach R, Michler GH, Chang Y- W. Macromol Rapid Commun 2005;26:728–33.
[151] Hong JH, Jeong EH, Lee HS, Baik DH, Seo SW, Youk JH. J Polym Sci. Part B Polym Phys 2005;43:3171–7.
[152] Chen H, Liu Z, Cebe P. Polymer 2009;50:872–80.
[153] Ko F, Gogotsi Y, Ali A, Naguib N, Ye H, Yang G, et al. Adv Mater 2003;15:1161–5.
[154] Kang MS, Shin MK, Ismail YA, Shin SR, Kim SI, Kim H, et al. Nanotechnology 2009;20. 085701/085701–085701/085705.
[155] Zhou W, Wu Y, Wei F, Luo G, Qian W. Polymer 2005;46:12689–95.
[156] Ji J, Sui G, Yu Y, Liu Y, Lin Y, Du Z, et al. J Phys Chem C 2009;113:4779–85.
[157] Kim GM, Michler GH, Pötschke P. Polymer 2005;46:7346–51.
[158] Sen R, Zhao B, Perea D, Itkis ME, Hu H, Love J, et al. Nano Lett 2004;4:459–64.
[159] Chen J, Li Z, Chao D, Zhang W, Wang C. Mater Lett 2008;62:692–4.
[160] Li Z, Huang H, Shang T, Yang F, Zheng W, Wang C, et al. Nanotechnology 2006;17:917–20.
[161] Dong H, Wang D, Sun G, Hinestroza JP. Chem Mater 2008;20:6627–32.
[162] Demir MM, Gulgun MA, Menceloglu YZ, Erman B, Abramchuk SS, Makhaeva EE, et al. Macromolecules 2004;37:1787–92.
[163] Jin W-J, Lee HK, Jeong EH, Park WH, Youk JH. Macromol Rapid Commun 2005;26:1903–7.
[164] Saquing CD, Manasco JL, Khan SA. Small 2009;5:944–51.
[165] Li D, Xia Y. Nano Lett 2003;3:555–60.
[166] Jose R, Kumar A, Thavasi V, Ramakrishna S. Nanotechnology 2008;19. 424004/424001–424004/424007.
[167] Lu X, Zhao Y, Wang C. Adv Mater 2005;17:2485–8.
[168] Guan H, Shao C, Wen S, Chen B, Gong J, Yang X. Inorg Chem Commun 2003;6:1302–3.
[169] Wang H, Tang H, He J, Wang Q. Mater Res Bull 2009;44:1676–80.
[170] Xin Y, Huang ZH, Peng L, Wang DJ. J Appl Phys 2008;105. 086106/086101-086106/086103.
[171] Viswanathamurthi P, Bhattarai N, Kim HY, Lee DR. Nanotechnology 2004;15: 320–3.
[172] Lu X, Zhao Y, Wang C, Wei Y. Macromol Rapid Commun 2005;26:1325–9.
[173] Demir MM, Soyal D, Unlu C, Kus M, Ozcelik S. J Phys Chem C 2009;113: 11273–8.
[174] Madhugiri S, Dalton A, Gutierrez J, Ferraris JP, Balkus Jr KJ. J Am Chem Soc 2003;125:14531–8.
[175] Li D, McCann JT, Xia Y. Small 2005;1:83–6.
[176] Li D, Xia Y. Nano Lett 2004;4:933–8.
[177] McCann JT, Li D, Xia Y. J Mater Chem 2005;15:735–8.
[178] Keng PY, Shim I, Korth BD, Douglas JF, Pyun J. ACS Nano 2007;1:279–92.
[179] Benkoski JJ, Bowles SE, Korth BD, Jones RL, Douglas JF, Karim A, et al. J Am Chem Soc 2007;129:6291–7.
[180] Nie Z, Fava D, Kumacheva E, Zou S, Walker GC, Rubinstein M. Nat Mater 2007;6:609–14.
[181] Xing S, Tan LH, Yang M, Pan M, Lv Y, Tang Q, et al. J Mater Chem 2009;19:3286–91.
[182] Srivastava S, Kotov NA. Soft Matter 2009;5:1146–56.
[183] DeVries GA, Brunnbauer M, Hu Y, Jackson AM, Long B, Neltner BT, et al. Science 2007;315:358–61.
[184] Krüger C, Agarwal S, Greiner A. J Am Chem Soc 2008;130:2710–1.
[185] Luo L-B, Yu S-H, Qian H-S, Zhou T. J Am Chem Soc 2005;127:2822–3.
[186] Zhan Y-J, Yu S- H. J Am Chem Soc 2008;130:5650–1.
[187] Lu G, Li C, Shen J, Chen Z, Shi G. J Phys Chem C 2007;111:5926–31.
[188] Cong H-P, Yu S- H. Curr Opin Colloid Interface Sci 2009;14:71–80.
[189] Jin M, Kuang Q, Jiang Z, Xu T, Xie Z, Zheng L. J Solid State Chem 2008;181:2359–63.
[190] Munoz-Rojas D, Oro-Sole J, Ayyad O, Gomez-Romero P. Small 2008;4:1301–6.
[191] Zhang S, Zhu H-Y, Hu Z-B, Liu L, Chen S-F, Yu S- H. Chem Commun; 2009:2326–8.
[192] Huang K, Zhang Y, Long Y, Yuan J, Han D, Wang Z, et al. Chem.–Eur J 2006;12:5314–9.
[193] Xiong S, Fei L, Wang Z, Zhou HY, Wang W, Qian Y. Eur J Inorg Chem; 2006:207–12.
[194] Yang Y, Nakazawa M, Suzuki M, Shirai H, Hanabusa K. J Mater Chem 2007;17:2936–43.
[195] Yang Y, Nakazawa M, Suzuki M, Kimura M, Shirai H, Hanabusa K. Chem Mater 2004;16:3791–3.
[196] Li M, Mann S. Angew Chem. Int Ed 2008;47:9476–9.
[197] Rambaud F, Valle K, Thibaud S, Julian-Lopez B, Sanchez C. Adv Funct Mater 2009;19:2896–905.
[198] Llusar M, Sanchez C. Chem Mater 2008;20:782–820.
[199] Sanchez C, Rozes L, Ribot F, Laberty-Robert C, Grosso D, Sassoye C, et al. Comptes Rendus Chim 2010;13:3–39.
[200] Yuan J, Schmalz H, Xu Y, Miyajima N, Drechsler M, Möller MW, et al. Adv Mater 2008;20:947–52.
[201] Yuan J, Gao H, Schacher F, Xu Y, Richter R, Tremel W, et al. ACS Nano 2009;3:1441–50.

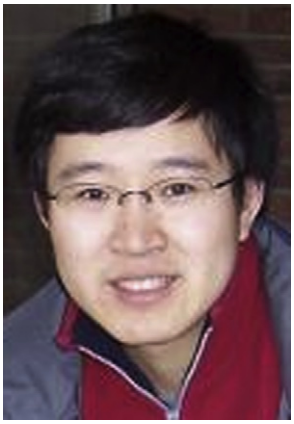

Jiayin Yuan studied chemistry at the Shanghai Jiao Tong University, China, and the University of Siegen, Germany. In 2009, he received his Ph.D. under the supervision of Prof. Axel H. E. Müller at the University of Bayreuth, Germany. Currently, he holds a post-doctoral scholarship in the Max Planck Institute of Colloids and Interfaces in Potsdam, Germany, working with Prof. Markus Antonietti.

Axel H. E. Müller obtained his Ph.D. in 1977 at the Johannes Gutenberg University in Mainz, working with G. V. Schulz. Since 1999 he has been professor and chair of Macromolecular Chemistry at the University of Bayreuth. In 2004 he received the IUPAC MACRO Distinguished Polymer Scientist Award. He is a Senior Editor of *Polymer*. His research interest focuses on the design of well-defined polymer structures by controlled/living polymerization techniques and on self-organized organic and hybrid nanostructures obtained from them.